COMPARISON OF SHEAR-WAVE VELOCITIES MEASURED FROM MICROTREMOR ARRAY STUDIES AND SEISMIC CONE PENETROMETER DATA IN PERTH W.A.

MICHAEL W. ASTEN[1], TREVOR DHU[2], ANDREW JONES[2] AND TREVOR JONES[2]
MONASHUNIVERSITY[1] AND GEOSCIENCE AUSTRALIA[2]

AUTHORS:

Michael Asten is a Principal Research Fellow at Monash University part-time, and is also a consulting geophysicist and Partner with Flagstaff Geo-Consultants, Melbourne. He majored in Physics, Geology and Geophysics at the University of Tasmania, and gained a PhD in geophysics from Macquarie University on the topic of using microseismic waves as a tool for studying sedimentary basins. In 1977 he took up a two-year appointment lecturing and coordinating an MSc (geophysics) programme in Nigeria. He then joined BHP Minerals in 1979 and worked in coal and base-metal exploration in Australia, East Africa and North America, with particular emphasis on geophysical research issues. He initiated a numerical modelling project in in-seam (coal) seismic modelling which became a standard tool in interpretation of commercial surveys. In the last decade he has specialised in electromagnetic and gravity exploration methodologies for mineral exploration, and is author or co-author of 79 technical papers. He is collaborating with Geoscience Australia, University of Melbourne, and the US Geological Survey in the development of passive seismic methods for geotechnical and site classification tasks. He was a co-recipient of the CSIRO Medal for External Research in 2000 and co-recipient of the ASEG Graham Sands Award in 2001, (both of these for development of the "Falcon" airborne gravity gradiometer).
Email: masten@mail.earth.monash.edu.au

Trevor Dhu is a geophysicist with the Minerals and Geohazards Division of Geoscience Australia. Trevor's current research is focused on the calculation of regolith site amplification factors for Australian conditions. He is also interested in the use of microtremor data for the delineation of regolith site classes in regions with limited geotechnical and geological data.

Andrew Jones is a research scientist with Geoscience Australia. He is also currently undertaking a PhD at the Earth Sciences Department, University of Queensland. His research interests are ancient glacial sedimentary deposits, modern coastal and marine geology, and the application of earth sciences to risk assessment in Urban Centres.

Trevor Jones is the Leader of Geoscience Australia's Cities and Critical Infrastructure Project in the Risk Research Group. His research interests include the development of Australian infrastructure damage models and economic loss models for natural hazards and other possible impacts. He is currently active in assessing the risks to Perth from natural hazards including earthquakes.

ABSTRACT:

Geoscience Australia is currently mapping and classifying the regolith in Perth (W.A.) for use in an earthquake risk assessment of the region. This classification is based on a combination of seismic cone penetrometer tests (SCPTs), supplemented with microtremor horizontal/vertical spectral ratio studies and published borehole data. This paper compares shear-wave velocities from SCPTs with shear-wave velocities derived by measuring microtremor phase velocities using small seismic arrays. Processing the array data using the multi-mode spatially averaged coherency (MMSPAC) method proves effective in providing direct measurements of sand/clay thickness and a shear-wave velocity profile which is comparable with SCPT measurements. The shear-wave velocities derived from microtremor array measurements are found to be within 10% of the SCPT estimates in the top 30 m of sand/clay. The array data is able to correctly identify low-velocity soft clays under sands. The method is also effective in regions where a surficial layer of calcareous sandstone would typically preclude SCPT measurements.

Paper No. 12

1. INTRODUCTION

The City of Perth (W.A.) is at risk of earthquake damage due to its proximity to the seismically active zone to the east of the Darling Fault combined with the region's regolith (soils, geological sediments and weathered rock). The Perth region is covered by relatively thick regolith material which has low seismic velocities, and has the potential to amplify the ground shaking experienced during an earthquake. The city's regolith is currently being modelled by Geoscience Australia, using a combination of seismic cone penetrometer tests (SCPTs), published boreholes and microtremor horizontal/vertical spectral ratio studies (HVSR) similar to that described by Nakamura (1989).

In this paper we report two examples where we obtain shear-wave velocity vs. depth profiles for the top hundred metres of the earth using the microtremor method (MTM). Shear velocities derived from the MTM supplement the HVSR and SCPT data, and in many cases are arguably sufficiently precise to present an alternative non-invasive method for acquisition of shear-wave velocity profile data.

2. THE FIELD AREA

As part of this study, microtremor data was acquired from five sites along a 20 km east-west transect of Perth's northern suburbs (Figure 1). Three sites (1,2 and 4) have SCPT measurements within 100 m of the study site and all sites have a drill-hole within 1000 m of the site. Due to the length restrictions, this paper only considers results from Sites 4 and 2, while a more detailed discussion of all sites is given in Asten (2003). Sites 4 and 2 were selected for this paper as they demonstrate the capabilities of the MTM for two distinct regolith styles within the Perth region.

3. PHASE VELOCITIES FROM MICROTREMORS

The MTM used here for estimating shear-wave velocity was proposed by Aki (1957) and has been reviewed by many authors (eg. Tokimatsu, 1997; Asten, 2001; and Okada, 2003). Microtremors are the background movement of the earth attributable to non-seismic sources. In the frequency band of interest in this study (1 to 30 Hz), sources are principally cultural noise such as vehicle traffic and industrial machinery. For studies in metropolitan areas, the MTM is especially useful as the seismic noise which degrades active seismic methods (such as seismic reflection and refraction surveys) provides a plentiful source of energy for passive seismic methods.

The microtremor seismic energy detected by vertical-component geophones propagates principally as fundamental-mode Rayleigh (surface) waves.The phase velocity of propagation is dependent mainly on shear-wave velocity (and less so on compressional velocity and density) of the underlying regolith. The velocity of propagation is a function of period; long periods have long wavelengths which are affected by rock properties deeper in the earth, while short periods have short wavelengths and are affected by rock properties at correspondingly shallower depths. In the MTM, we measure phase velocity over a range of frequencies and invert these to a layered-earth model by iterative fitting of observed and modelled dispersion data.

Numerous seismic sources contribute energy to the MTM at any instant of time, hence the direction of wave propagation is undefined. Consequently, standard ray-path methods used in conventional seismology are not appropriate for this technique. Instead, we use spatially-averaged coherencies (SPAC) computed using a small circular seismic array as shown in Figure 2. The spatially averaged coherency for a single-mode surface wave observed with a circular seismic array is given by

$$ave\ c(f) = J_0(kr) = J_0(2\pi f r / V(f)), \qquad \text{-----(1)}$$

where *ave c(f)* is azimuthally-averaged coherency,
f = frequency, J_0 is the Bessel function of zero order,
k is the scalar wavenumber, $V(f)$ is the required phase velocity dispersion curve, and r is the station separation in the circular array (Aki, 1957).

The seven-station circular array shown in Figure 2 allows estimates of SPAC over three different radial distances r, 1.7r and 2r. Estimating coherencies simultaneously at three separations gives sufficient redundancy to identify frequencies where energy is propagating in two modes simultaneously (such as the fundamental and first higher modes), and to solve for the two phase velocities and energy partition coefficient (Asten, 2001). However, we only consider fundamental-mode Rayleigh-wave energy in this paper.

The classical method of analysis is to fit coherencies at each frequency to a Bessel function curve, and thus obtain a value for phase velocity $V(f)$ (Okada, 2003; Ohori, 2002). The phase velocity data is then fitted to modelled phase-velocity dispersion curves either by iterative forward modelling, or by inversion algorithms. In this work we use an alternative procedure following Asten et al. (2002) whereby we compute modelled phase velocity dispersion curves, compute modelled coherency vs frequency curves *via* eqn (1), and then fit observed and model coherencies by iterative modelling. The modelled dispersion curves are obtained for layered earths by using routines published by Herrmann (2001). This approach is similar to that used by Chouet et al (1998), proves more robust than the classical SPAC methodology, and facilitates recognition of multi-mode Rayleigh-wave propagation if present. For this reason we term it the multi-mode SPAC (MMSPAC) method.

4. RESULTS

In each example discussed here, field data was acquired with two circular arrays of radii 25 m and 50 m. The modeling for Site 4 was carried out with the aid of shear-wave velocities from SCPT. However, the SCPT data for Site 2 was withheld during the first phase of the interpretation process, thus allowing for a blind study of the interpretation process.

Site 4
Figure 3 presents observed and modelled coherencies for an array at Site 4 (Warwick). This site has an SCPT measurement within 50 m of the array, and a drill-hole 1 km south of the site. Figure 4 shows a shear-wave velocity model constructed from the SCPT and drill-hole data, together with a modified result obtained by iterative fitting to gain the coherency match shown in Figure 3. The fit of field microtremor array coherencies to the modelled fundamental Rayleigh mode R0 (dashed line in Figure 3) is good over the range 0.5 to 10 Hz, with the exception that the point at 1.8 Hz gives a better fit to modelled R1 higher-mode energy (dotted line) for all data files acquired at this site. The two shear-wave velocity models (Figure 4) obtained from SCPT and microtremor data are a close match except for layer 3 where the microtremor data resolves a shear velocity which is 20% lower than that derived from the SCPT data.

Site 2 – with low-velocity clay below sands
Figures 5 and 6 present shear-wave velocity vs. depth profiles and observed SPAC coherencies at Site 2 (Crimea Ten Park). The data from this site was initially modelled using depths obtained from a drill-hole, and velocities based on estimates related to sand/clay content. The drill-hole section is notable for containing a thickness of 23 m of clays underneath 53 m of mainly sands, and also for having a shallow thin layer of calcareous cemented sand or "coffee rock" at a depth of 2 m. These features raise the question whether the microtremor method can identify an inversion in the velocity-depth profile. Results of iterative fitting of the SPAC coherency data in Figure 6 shows that the velocity inversion associated with the thick basal clay layer is resolved.

However, the modelling shows no indication of the existence of the thin band of near-surface coffee-rock.

Figure 7 shows a new starting model for Site 2 based on the SCPT data, (supplied after completion of the previous interpretation). The SCPT penetrated only to a depth of 18.8 m, presumably halted by coarse sands. The velocity model yielded by SCPT alone is plotted in Figure 7 (partially obscured by over-printing by the heavy dashed line) and gives a very poor fit of modelled and observed SPAC data (not shown). This result is in part expected due to the erroneously-shallow basement yielded by the SCPT.

However, when the SCPT velocities to 18 m are combined with layer thickness to 75 m yielded by the drill hole data, the resultant velocity model (Figure 7, dashed curve) is very close to that derived without benefit of the SCPT data. For depths 4 to 18 m the SCPT shear velocities correspond exactly with SPAC-derived velocities, while at shallow depths 0 to 5 m, the former are about 25% higher than velocities required for fitting the SPAC data. A discrepancy at such shallow depths may be explicable due to the difficulty of identifying shear arrivals in SCPT measurements at very shallow depths. The existence of the low-velocity layer corresponding to the basal clay (below the depth of SCPT measurements) is confirmed in the SPAC data. An important discrepancy between SCPT and SPAC results relevant to geotechnical engineering applications is that the SPAC data does *not* resolve any indication of the thin harder layer (presumably coffee rock) which was detected by the SCPT at a depth of 5 to 6 m (Figure 7).

Figure 8 shows the observed and modelled HVSR ratios for the site. The important resonance peak in observed data is at period 0.8 sec, but is surprisingly weak. Coupled with the difficulty in obtaining SCPT data to the base of sands and clays, this weakness provides an example where HVSR plus SCPT may produce an incomplete classification of site conditions, whereas the microtremor data is able to explicitly resolve a shear-wave velocity profile.

5. CONCLUSIONS

The application of the MMSPAC method to data from Perth has demonstrated that shear-wave velocity profiles derived by iterative fitting of observed and modeled coherencies have comparable accuracy to SCPT measurements. This has been demonstrated both by direct comparison and by a blind study where SCPT data has been disclosed after completion of a shear-wave velocity interpretation. The microtremor method has the notable advantages over SCPT measurements that it is uses purely passive seismic sources, is non-invasive, and yields shear-wave velocity estimates at depths below the limits imposed by coarse sands or gravels on SCPT measurements.

As mentioned earlier, length constraints have limited the number of sites described in this paper. However, the remaining three sites are described in detail in Asten (2003) and had similar quality results to the two sites described here. Moreover, the ability of the MTM to identify low-velocity sediments under higher-velocity sediments was confirmed at one of these sites where hard calcareous sandstone overlies sands, and precludes use of SCPT methods Asten (2003).

The ability of the MTM to derive a shear-wave velocity profile extends to cases where the HVSR method fails to produce significant spectral peaks. MTM therefore provides greater certainty in site classification than the HVSR method in cases where shear-wave velocity contrasts are low or gradational.

6. REFERENCES

Aki, K. (1957) Space and time spectra of stationary stochastic waves, with special reference to microtremors. Bull, Earthq. Res. Inst, Vol 35, pp 415-456.

Asten, M.W. (2001) The Spatial Auto-Correlation Method for Phase Velocity of Microseisms – Another Method for Characterisation of Sedimentary Overburden: in Earthquake Codes in the Real World, Australian Earthquake Engineering Soc., Proceedings of the 2001 Conference, Canberra, Paper 28.

Asten, M.W., Lam, N., Gibson, G. and Wilson, J. (2002) Microtremor survey design optimised for application to site amplification and resonance modelling, *in* Total Risk Management in the Privatised Era, edited by M Griffith, D. Love, P McBean, A McDougall, B. Butler, Proceedings of Conference, Australian Earthquake Engineering Soc. , Adelaide, Paper 7.

Asten, M.W. (2003) Research into microtremor phase velocity techniques for earthquake hazard assessment – Velocity models, spectra, and comparison with SCPT data for the Perth (W.A.) northern suburbs. Report to Geoscience Australia. Monash University, August 2003.

Chouet, B., De Luca, G., Milana, G., Dawson, P., Martini, M., and Scarpa, R. (1998) Shallow velocity structure of Stromboli Volcano, Italy, derived from small aperture array measurements of Strombolian tremor. Bull. Seism.Soc. Am. Vol 88 pp. 653-666.

Herrmann, R.B. (2001) Computer programs in seismology - an overview of synthetic seismogram computation Version 3.1, Department of Earth and Planetary Sciences, St Louis Univ.

Nakamura, Y. (1989) A method for dynamic characteristics estimation of subsurface using microtremors on the ground surface, Quarterly reports of the Railway Technical Research Institute Tokyo, Vol 30, pp 25-33.

Ohori, M., Nobata, A., and Wakamatsu, K. (2002) A comparison of ESAC and FK methods of estimating phase velocity using arbitrarily shaped microtremor arrays. Bull. Seism. Soc. Am. Vol. 92, pp. 2323-2332.

Okada, H. (2003) The Microseismic Survey Method: Society of Exploration Geophysicists of Japan. Translated by Koya Suto, Geophysical Monograph Series No. 12, Society of Exploration Geophysicists, Tulsa.

Satoh, T., Kawase, H., Iwata, T., Higashi, S., Sato, T., Irikura, K., and Huang, H. (2001) S-wave velocity structure of the Taichung basin, Taiwan, estimated from array and single-station records of microtremors. Bull. Seism. Soc. Am. Vol. 91, pp. 1267-1282.

Tokimatsu, K. (1997) Geotechnical site characterization using surface waves, *in* Earthquake Geotechnical Engineering, editted by Ishihara. Balkema, Rotterdam.

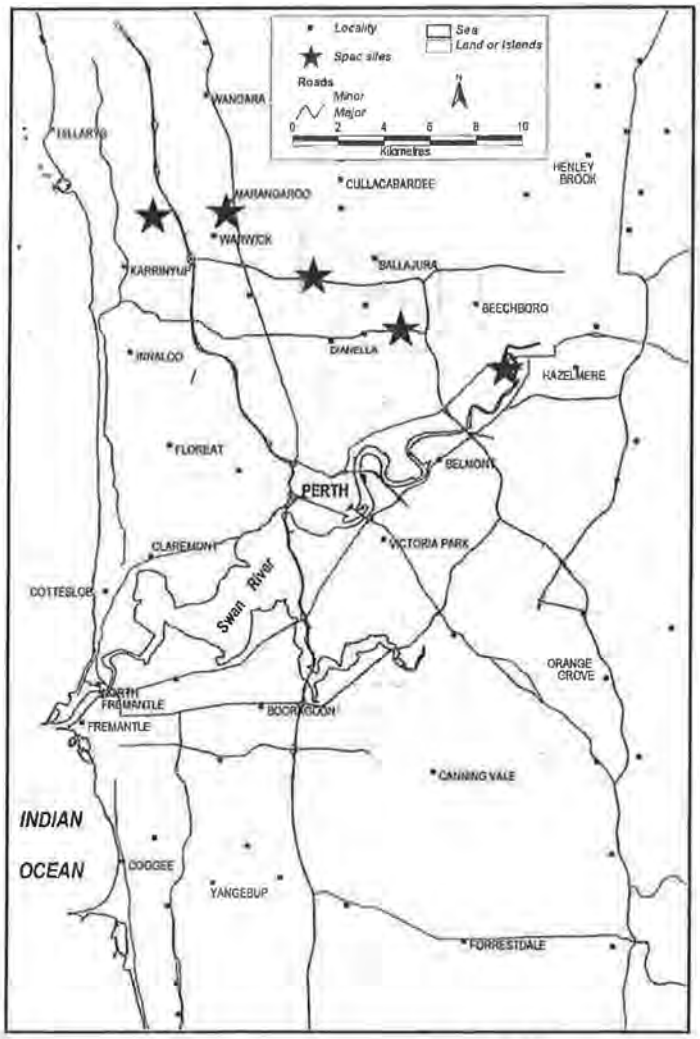

Fig. 1. Location of a profile of five microtremor array sites, northern suburbs of Perth (W.A.).

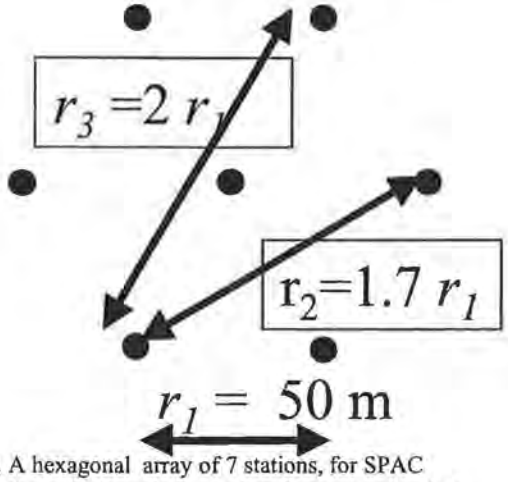

Fig. 2. A hexagonal array of 7 stations, for SPAC processing with three inter-station distances, allowing separation of dual modes of phase velocities at each frequency.

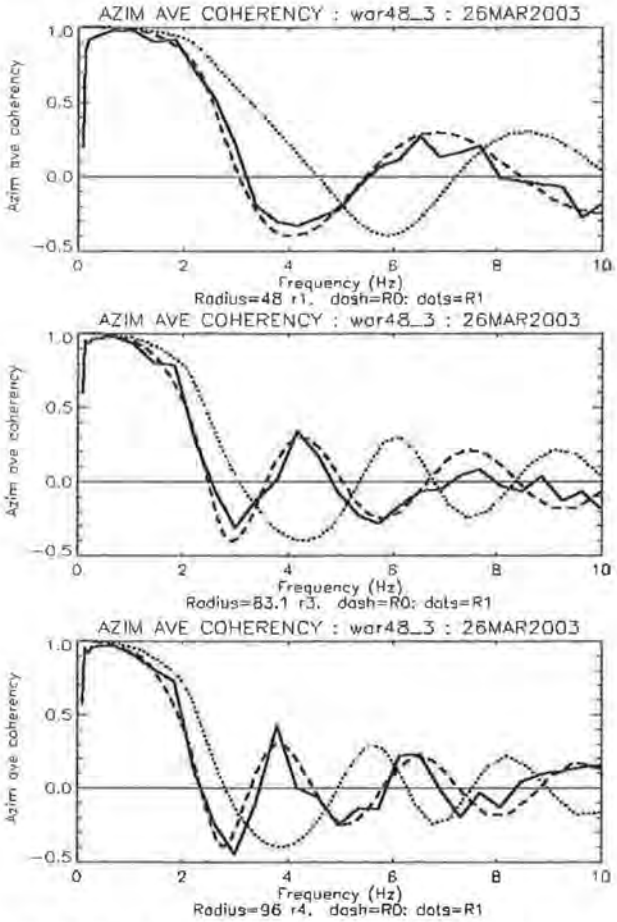

Fig. 3. Site 4: Observed coherencies for station separations 48, 83, 96 m, and modelled coherencies for the "best fit" model from Fig. 4. The fit for the fundamental Rayleigh mode R0 (dashed line) is good over the range 0.5 to 10 Hz. The point at 1.8 Hz fits R1 higher-mode energy (dotted line). Fitting of coherencies is performed simultaneously for data and model for the three station separations.

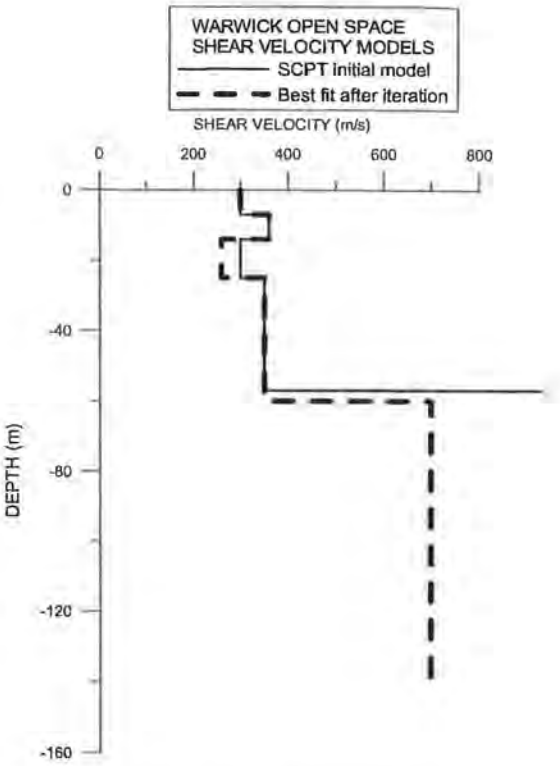

Fig. 4. Thin line is the initial model based on SCPT and a drill-hole.
Dashed line is the best fit after model iteration.
Velocities for the top 3 layers are resolved to +-10% or better.
Layer 3 is the only significant discrepancy between SCPT data and microtremor-derived shear velocity.

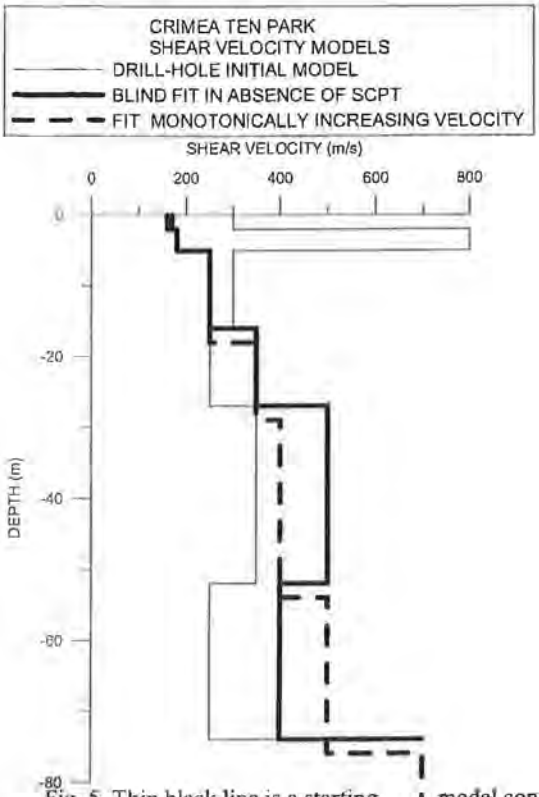

Fig. 5. Thin black line is a starting model constructed from borehole data without knowledge of SCPT data.
Heavy black is the best fit layered earth after iteration.
Dashed line is best fit using a monotonically increasing Vs profile.

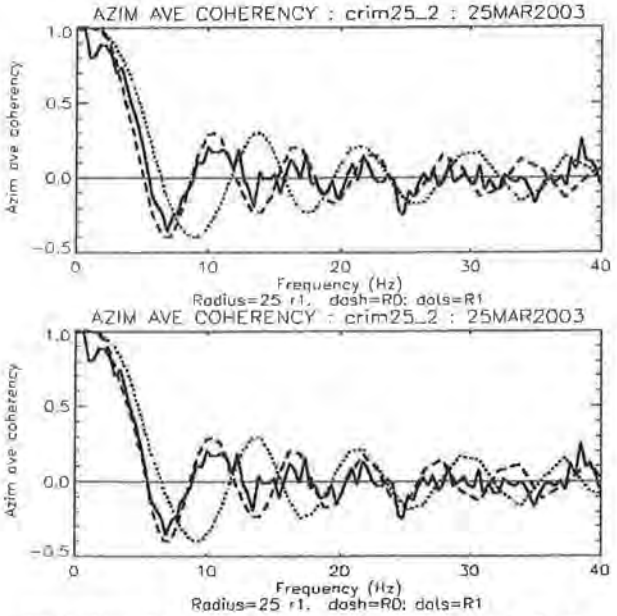

Fig.6. Site 2 Crimea Ten Park : Observed and modelled coherencies for station separation 25 m.

TOP: best fit using a monotonically increasing shear velocity with depth. Dashed line is the modelled fundamental mod.e

BOTTOM: best fit using the model with the low velocity layer shown in Fig. 5. In the second model, the fit is improved for frequencies 2-7 Hz. In each case, fitting of field and model coherencies was performed simultaneously for station separations of 25, 43.3 and 50 m, but only the 25 m data are shown here.

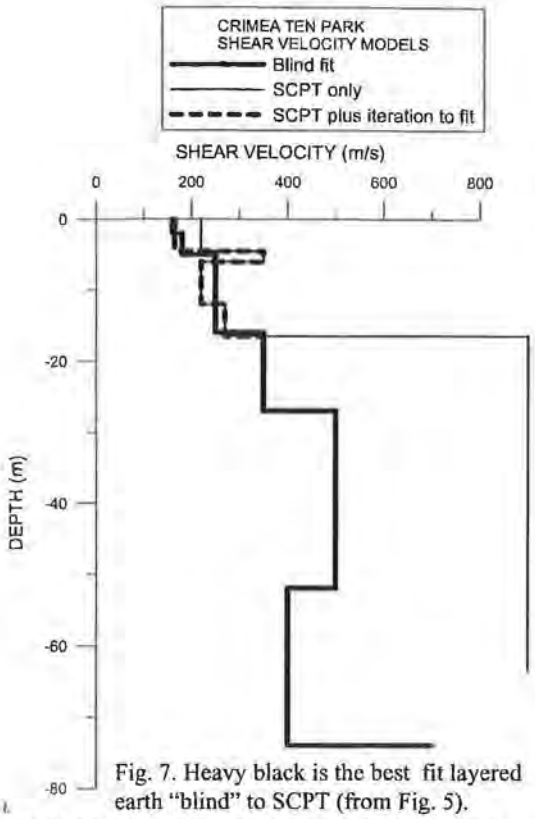

Fig. 7. Heavy black is the best fit layered earth "blind" to SCPT (from Fig. 5).
Thin line is a model derived from SCPT data only (apparent basement at 18.5 m). Dashed line is SCPT model combined with drill-hole data to 75 m, after iteration to fit SPAC data.

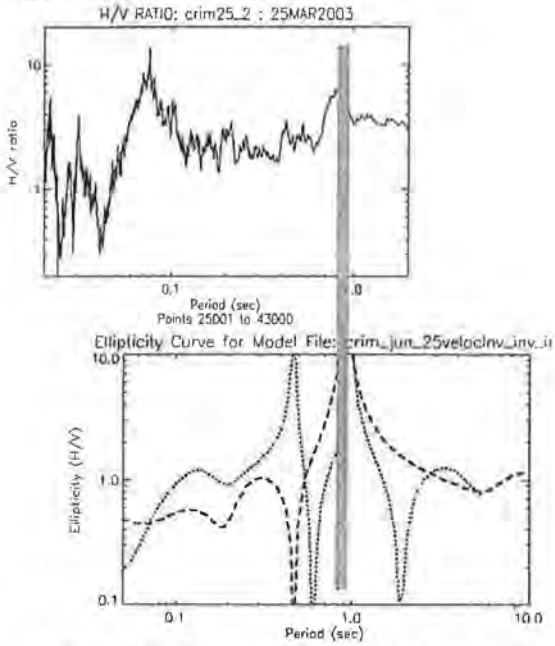

Fig. 8. Site 2 Crimea Ten Park. TOP: Observed H/V spectrum.

BOTTOM: H/V particle motion ellipticity fortwo modes, for .the "blind fit" layered-earth model of Fig. 7. Dashed line: particle motion for fundamental Rayleigh mode. Dotted line: 1st higher mode.

EARTHQUAKES IN DISSIMILAR TECTONIC REGIMES - COMPARISON STUDY OF SHALLOW EVENTS WITH SIMILAR MAGNITUDE

KEVIN MCCUE [1] AND CVETAN SINADINOVSKI[2]
AUSTRALIAN SEISMOLOGICAL CENTRE[1], PO BOX 324, JAMISON CENTRE 2614 ACT, AUSTRALIA
GEOSCIENCE AUSTRALIA[2], GPO BOX 378, CANBERRA 2601 ACT, AUSTRALIA

AUTHORS:

Kevin McCue is Director of the Australian Seismological Centre, a Fellow of IEAust, and co-founder with Charles Bubb of the Australian Earthquake Engineering Society.

Cvetan Sinadinovski is a seismologist at Geoscience Australia who graduated from the famed Mohorovicic School in Macedonia and completed his PhD in Geotomography at Flinders University.

ABSTRACT

The lack of local data for earthquake design in Australia forces engineers to use spectra and time histories recorded elsewhere. One area with a significant database of strong motion records is the Eastern Mediterranean which is characterised by strong regional compression similar to that in southwestern Australia.

The suitability of the eastern Mediterranean as a source of applicable accelerograms for Australia can be tested by comparing macroseismic information collected following similar sized earthquakes in each region. The magnitude Ms 6.0 earthquake of 2 June 1979 in WA was a large shallow event, its epicentre near the town of Cadoux which suffered significant damage but no deaths. The earthquake was felt over a radius of about 500 km and a well defined isoseismal map was subsequently drawn up. It was recorded on an analogue accelerograph at an epicentral distance of about 90 km.

On 26 July 1963 a shallow magnitude Ms 6.0 struck Skopje, capital of Macedonia. It too caused considerable damaged resulting in 1,066 fatalities. A comprehensive macroseismic study resulted in a detailed isoseismal map but in this case there were no accelerographs installed in Macedonia.

Comparison of the macroseismic data from the two earthquakes, nearly identical in terms of their size and mechanism, shows that they occurred in areas with different attenuative characteristics so that the Macedonian earthquake spectra are quite different from those in Australia rendering them unsuitable for direct use in design or in codes in Australia. The import of such data may lead to a serious underestimation of pga or spectral acceleration in regions with low attenuation, and consequently can not be directly substituted in the development of the building code in the absence of local instrumental recordings.
For good measure we looked at a magnitude Ms 6.0 earthquake in Queensland and then compared accelerograms of P phases recorded on rock during magnitude M5.5 earthquakes in Eastern and Western Australia.

1. INTRODUCTION

The Australian continent is within the Indo-Australian Plate and its seismicity is typically intraplate. Oral history records for Sydney go back to 1788 but every other city has a shorter record. Seismographs were installed in Australia as early as 1888 and according to the Geoscience Australia earthquake database some twenty earthquakes were recorded in the 20th century with magnitudes of 6.0 or greater. Records indicate that on average there are 2 to 3 earthquakes per year with a magnitude of 5.0 or more (M^{c}Cue *et al.*, 1995).

In contrast to the intraplate setting of Australia, Macedonia is situated in the Mediterranean seismic belt, a complex boundary between the African and Eurasian plates characterised by shear and compression. This area has historically experienced moderate to large shallow earthquakes and the area around Skopje is considered the most active part of the zone (Hadzievski, 1976).

The ancient city of Skupi which is 4 to 5 km north-west of the present Skopje was destroyed by an earthquake in 518 A.D. In 1555 another earthquake is said to have demolished a part of the town of Skopje and again in 1921, this time by a series of shocks.

On 26 July 1963, at 04:17 GMT (early morning local time), North Macedonia was shaken by a severe local earthquake. The epicentre computed by a number of European seismological stations was about 5 km north of the centre of Skopje. The average magnitude of the main shock from macroseismic methods was M 6.1 (Ambraseys, 1968) whilst NOAA assigned it a magnitude of Ms 6.0. The earthquake was assigned a crustal depth but no surface faulting was observed and the exact mechanism is unknown.

In this study we shall compare the isoseismal maps of the Skopje 1963 earthquake with a similar sized event which took place in Australia in a dissimilar tectonic regime. We have chosen the Cadoux event of magnitude Ms 6.0 which occurred in 1979 in Western Australia (Gregson and Paull, 1979). The focus was shallow as evidenced by significant surface faulting which also indicated a reverse faulting mechanism.

In addition we have undertaken a preliminary comparative study of two magnitude 5.5 events, one in Western Australia the other in Eastern Australia for which there is limited strong motion data.

2. DATA

Seismic intensity is by definition the degree of shaking at a specific place during a given earthquake. The degree of shaking is a rating assigned by an experienced observer using a descriptive scale called the intensity scale. In assessing the intensity it should always be recognised that it is open to subjective interpretation because it is not based on actual strong motion records. A variation in assigned intensity at any single location of as much as one intensity degree is quite common between observers. Different foundation conditions at the same distance from the epicentre can also modify the level of shaking.

For display purposes we have assumed similarity between the Modified Mercalli or MM scale and the Mercalli-Cancani-Sieberg or MCS scale. The maximum intensity of the main shock in the Skopje event was estimated between VIII to IX on both scales. At very short distances, the apparent intensity may vary dramatically as a result of foundation conditions and quality of construction as well as the mechanism of the event. No definitive visible faulting was observed near Skopje, perhaps disguised by the thick alluvial sediments, whilst the energy release in the near-field was consistent with movement of a small block structure (Ambraseys, 1968).

After the Skopje earthquake, the Seismological Institute in Belgrade and the Seismological Station in Skopje sent out about 5,800 questionnaires, out of which some 20% were returned. The macroseismic data have been evaluated and preliminary isoseismal map plotted (Fig. 1-a;

after P.Georgevski from the Seismological Station in Skopje). A second revised map (Fig. 1–b; D. Hadzievski, Director of Skopje Observatory) was published later.

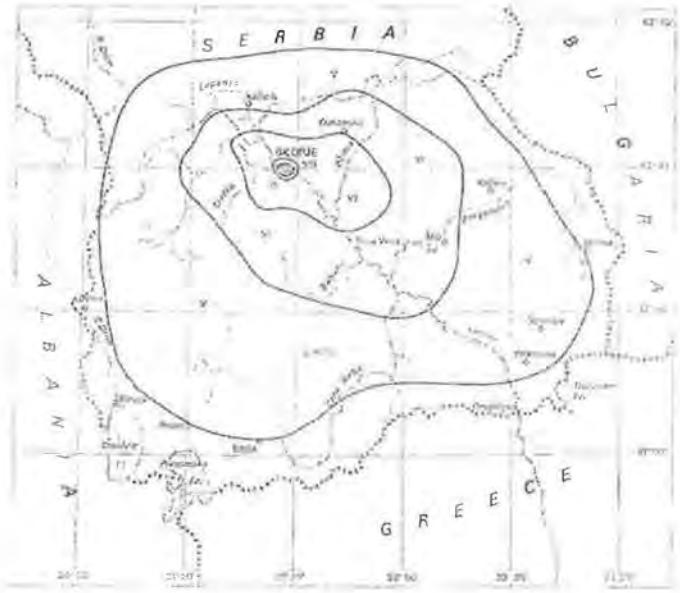

a) Preliminary isoseismal map of the main shock, 26 July 1963

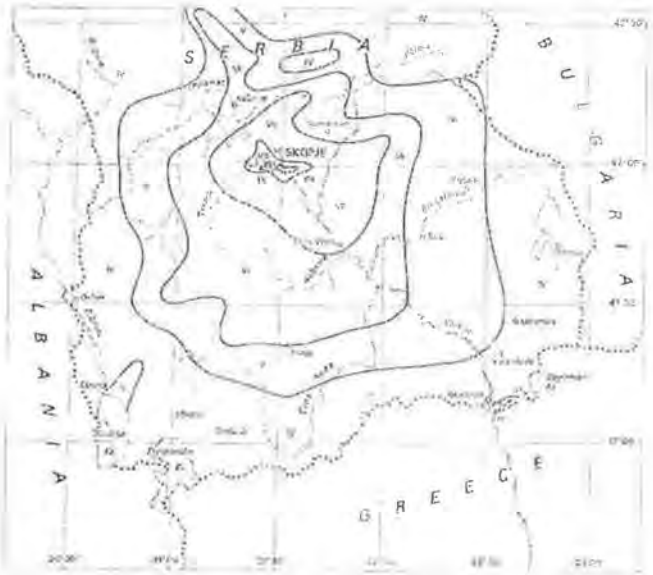

b) Revised isoseismal map of the main shock, 26 July 1963

Figure 1: Reproduced isoseismal maps of the Skopje earthquake (after Zátopek, 1968)

On 2 June 1979 a magnitude Ms 6.0 occurred at 5:48 pm local time near the small township of Cadoux in a farming area 180 km northeast of the State capital, Perth. Cadoux was wrecked but only one person was injured (Gregson, 1980). The isoseismal map of the larger region with enlargement of the epicentral area is shown in Figure 2 below.

ISOSEISMAL MAP OF THE CADOUX EARTHQUAKE, WESTERN AUSTRALIA 2 JUNE 1979

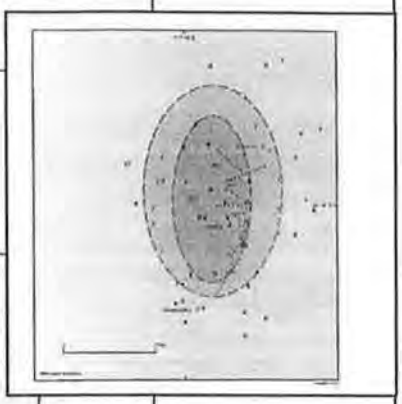

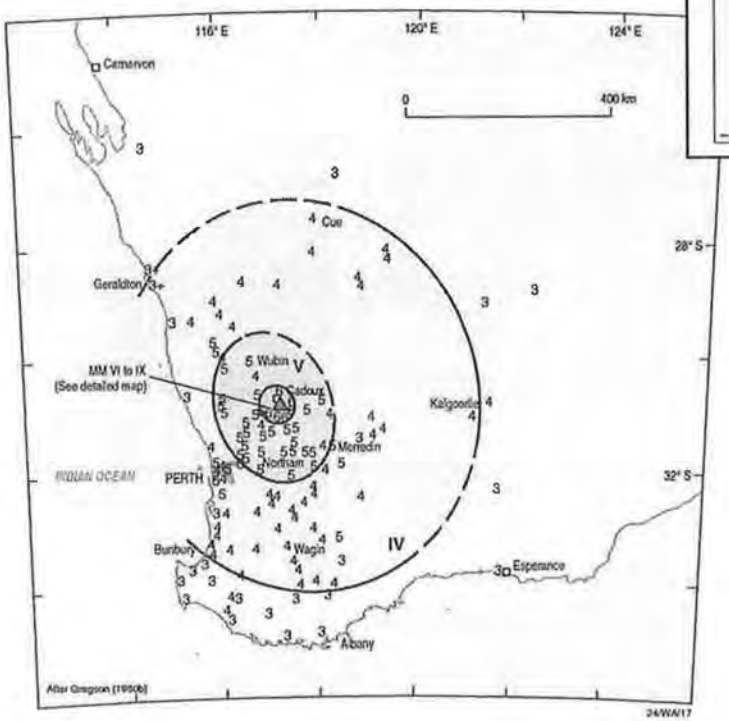

DATE: 2 JUNE 1979
TIME: 09:48:01.1 UT
MAGNITUDE: 6.2 ML(MUN), 6.2 Ms(BMR), 6.0 MB(GS)
LOCATION: 30.79° S, 117.16° E
DEPTH: 15 km

▲ *Epicentre*
IV *Zone intensity designation*
4 *Earthquake felt (MM)*
0 *Earthquake not felt*

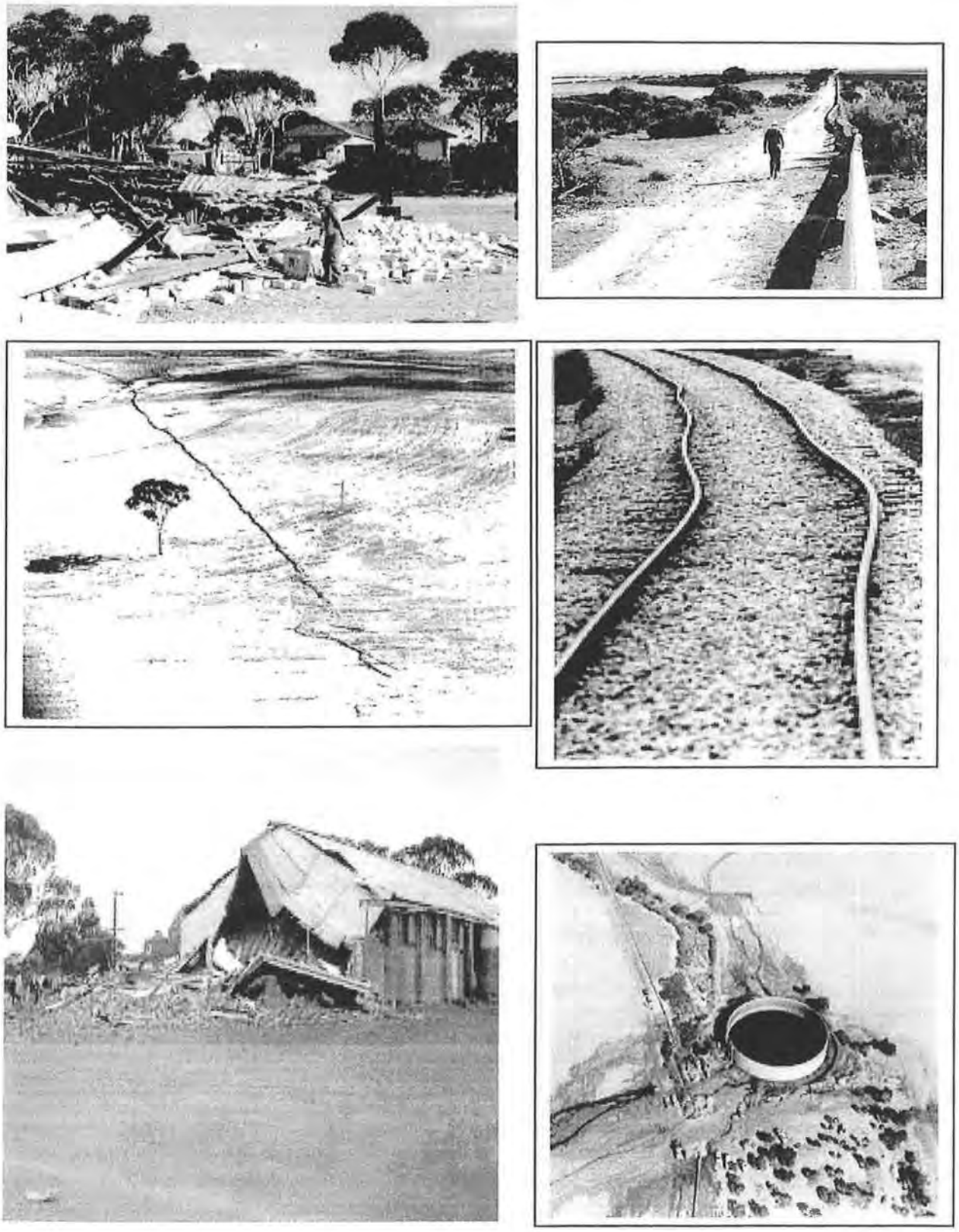

Figure 3: Images of destruction in the 1979 Cadoux WA earthquake; unreinforced masonry buildings, a section of surface faulting, buckled water pipeline and railway line, and a water tank which slid on its foundation breaking the connecting pipe, releasing most of the precious water.

3. METHODOLOGY

Subjective though it is, the macroseismic information summarised in an isoseismal map can be used to investigate useful parameters such as the focal depth and attenuation coefficients if actual recordings of strong ground shaking are not available. Such formulae as those developed by Köveslighethy (1907) are readily available. In the absence of records from local stations during the Skopje 1963 earthquake, the determination of its focal depth from records of distant stations was inevitably uncertain.

The maximum intensity of the main shock in the case of Skopje was assessed between VIII to IX on the MM scale, while the radius of perceptibility was about 240 km. The damage pattern was typical of a moderate sized, very shallow earthquake, striking a city whose buildings were constructed without consideration of earthquake loads. Zátopek (1968), taking the reported epicentral intensity and some common estimates for the coefficient of absorption, obtained a hypocentre depth of between 3 and 6 km, with an average value of 5 km.

One can also use formulae connecting the quantities of epicentral intensity and focal depth with the earthquake magnitude M obtainable both from instrumental and macroseismic data. Using the formulae of Kárnik (1969) a mean value of M 6.2 was found for the Skopje main event, while Shebalin's formula produced slightly smaller values. Thus, the ultimate value of magnitude based on macroseismic date averaged about M 6.1.

For the Cadoux case, members of the Mundaring Geophysical Observatory reported that the area of damaging intensities was about 300 km^2 and centred to the west of the earthquake's fault trace (Lewis *et al.*, 1981). The earthquake's fault plane determination indicates that the area of maximum intensity appeared on the surface projection of an east-dipping fault, although the depth of the hypocentre was not well constrained.

The isoseismal map survey showed that the Cadoux earthquake was felt clearly over a radius of 500 km (Fig. 2). The maximum modified Mercalli intensity of MM IX was observed adjacent to the earthquake fracture, and intensities MM VII or greater occurred up to 5 km from the surface fracture. Intensities in Perth ranged between MM IV and MM V.

Using the isoseismal map the area and its equivalent radius for each intensity can be determined. We measured those parameters for the Cadoux earthquake and compared them with the values found for Skopje (Zátopek A., 1968). Table 1 contains both Skopje and Cadoux calculations:

I_0	VIII	VII	VI	V
Skopje Area (km^2)	191	2682	8459	18333
Skopje $_{I, I-1}$ (km)	7.7	29.2	52.0	76.3
Cadoux Area (km^2)	314	707	3848	41548
Cadoux $_{I, I-1}$ (km)	10	15	35	115

Table 1: Epicentral distance and area calculations versus intensity

It can be seen that the area with maximum intensity was slightly larger in the Cadoux event in comparison with the Skopje event. The curves show that both events were very shallow but that attenuation of seismic energy was greater in Macedonia than Western Australia as might have been expected.

4. ATTENUATION IN WESTERN AUSTRALIA, QUEENSLAND AND MACEDONIA

Figure 4 shows the radius versus intensity difference for the two events. The radius for isolines with intensities VIII to IX was evidently larger in the case of Cadoux in comparison

to the Skopje event. That is no surprise knowing that the 1979 Cadoux earthquake produced a fault scarp 17 km long with an average vertical and horizontal displacement of 0.3 m.

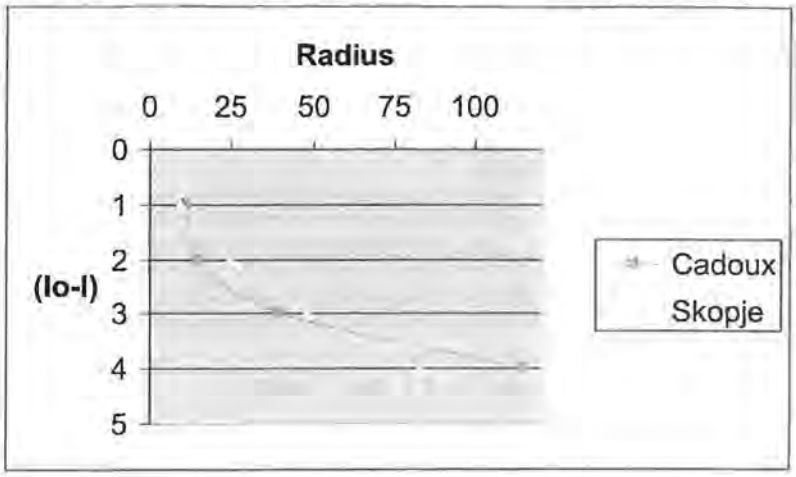

Figure 4 Radius of isoseismals versus intensity difference for the two earthquakes

Intensity dropped off faster beyond 50 km in the Skopje region than in the Cadoux region. While the near field intensities are strongly influenced by focal depth (obviously less than 10 km for both earthquakes), the far field observations are mainly a reflection of the attenuative characteristics of the local crust. We speculate that the rapid decrease in intensity within 50 km of the epicentre in Cadoux was due to the surface faulting.

The pattern of aftershocks between Skopje and Cadoux is quite different. The strongest aftershock in Skopje occurred on 26 July 1963 at 04:52 GMT and was estimated by USGS as magnitude 4.2. A more detailed study covering the six months after the main shock was compiled by D. Hadzievski. Daily records of aftershocks in August 1963 show about 23 events with intensity V with only a further six in the following months.

In the month following the Cadoux earthquake there were many aftershocks, two of which had magnitudes greater than 5 that were widely felt throughout the southwest of Western Australia. Most of the other aftershocks were of small magnitude, but 42 aftershocks were of M 3.0 or greater. In the six months after the main event, a further 14 tremors with magnitude 3.0 or more were recorded.

A number of indirect estimates of the dominant, but not necessarily maximum acceleration during the Skopje main shock gave values between 0.38 *g* and 0.48 *g*. Those values were computed from a number of overturned trolleys running on a narrow-gauge rail, from some masonry walls on the ground floor of unfinished houses, and from the movement of the furniture on the basement and ground floors in various apartments (Ambraseys, 1968). The duration of the destructive part of the shaking from the main Skopje event was very brief, probably 2 to 5 seconds.

Four accelerographs in the Meckering area, 90 km from Cadoux, recorded maximum accelerations of approximately 0.01*g*. At Mundaring Weir, 120 km from Cadoux, the accelerograph recorded maximum east, vertical, and north component accelerations of 0.04, 0.02, and 0.01*g* respectively (Everingham *et al.*, 1982).

We have also made a preliminary study of a magnitude Ms 6.0 earthquake in Queensland in 1918 and other smaller events in WA. Interestingly the attenuation in WA and Queensland appear to be similar, and the attenuation characteristics of each of the three WA earthquakes we have studied are very similar, regardless of their magnitude.

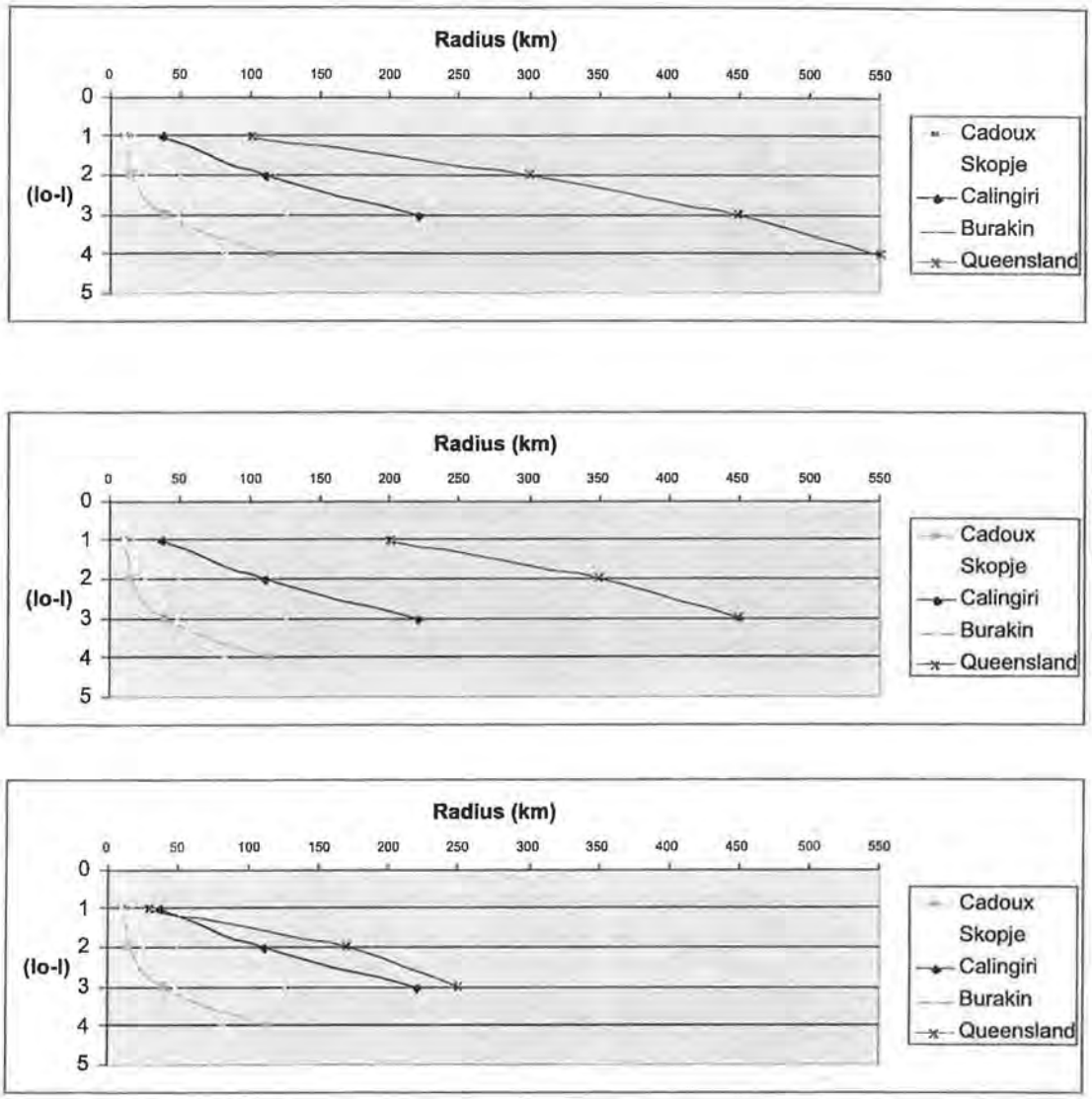

Figure 5 The top figure shows averaged radii, the lower two the north/south and east/west radii respectively.

5. STRONG MOTION DATA NSW AND WA

Three weeks after the December 1989 Newcastle NSW earthquake, a similar sized earthquake occurred on the opposite side of the continent near Meckering Western Australia. The P-wave of each event was recorded on accelerograms at similar distances (near 100 km) on rock and a Fourier analysis of the three components of each phase is shown below. The S-wave was unfortunately not recorded on the Sydney recorder.

The intensities were similar at the recorder sites but the spectra of the P phases at least are very different, the higher frequencies propagating further in WA. The peak in the Sydney record is in the bandwidth 10 to 25 Hz whereas that in WA is in the range 18 to 35 Hz. This is tantalising evidence for a real difference between the damage potential of Eastern and Western Australia though it would have been more useful if the shear wave too had been recorded. More data are required which will only become available in a reasonable time if many more accelerographs are installed in Australia.

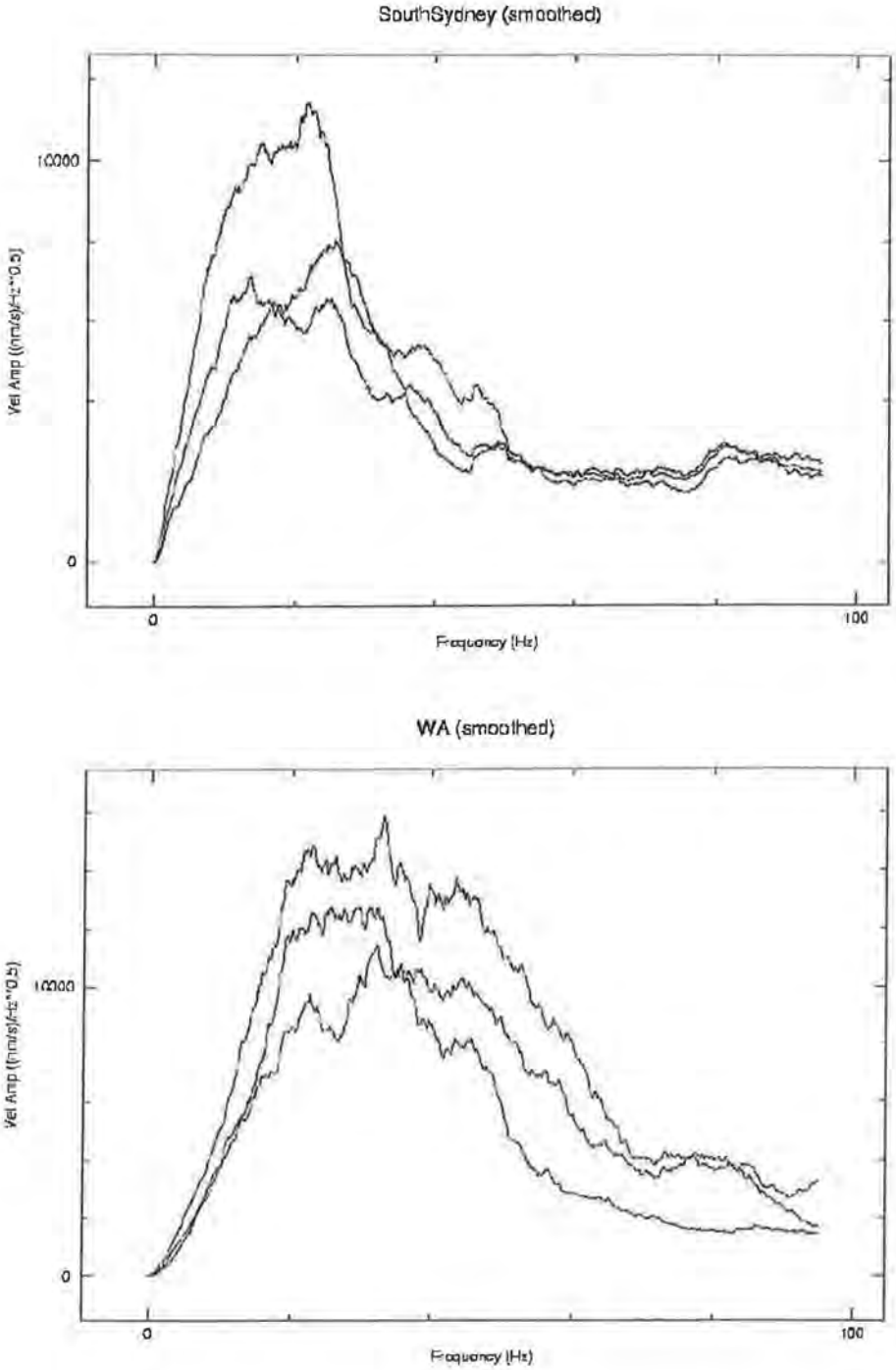

Figure 6 Spectra for the P-wave of similar sized earthquakes near Sydney (top) and Perth in 1989 and 1990 respectively.

CONCLUSION

In 1963 the city of Skopje, capital of Macedonia was devastated by earthquake (M=6.1, I_{max}=IX MCS). The earthquake damaged 85% of the buildings in the city and caused a loss of about 1,066 lives. The direct economic losses were estimated at 1 billion 1963 US$, or 15% of the GNP of the country. The damage was mainly attributed to the lack of an appropriate building code and resulting inadequate methods of construction.

For comparison we examined a similar size earthquake (magnitude Ms 6.0) that occurred on 2 June 1979 near Cadoux, some 180 km northwest of Perth. The township of Cadoux was

wrecked but only one person was injured. The earthquake damaged or wrecked buildings and structures in the area within approximately 35 km of Cadoux. Roads, pipes, and power and railway lines were damaged by the strong shaking and significant surface faulting was observed. Information from insurance and Government Works Department sources indicate that damage costs amounted to around $3.8 million (1979 prices). The difference in human casualties and damage bill can be attributed primarily to the sparsity of the population in Australia.

No strong motion seismographs had been installed in Macedonia in 1963, and all knowledge about the ground movements had to be based on macroseismic observations. Four accelerographs recorded the Cadoux 1979 event but all of them were too distant from the epicentre for use in developing design response spectra. Comparison of macroseismic data shows that one needs to exercise caution when using data from dissimilar seismotectonic regimes, as they manifest different characteristics. The imported data may lead to serious underestimation or overestimation of peak ground acceleration and consequently should not be used to develop building code in the absence of local instrumental recording, even when the mechanism and focal depths are comparable.

REFERENCES

Ambraseys, N.N., 1968 – The Skopje earthquake 1963, *Report of the UNESCO Technical Assistance Mission,* Amsterdam, 1968.

Everingham, I.B., McEwin, A.J., and Denham, D., 1982 – Atlas of Isoseismal Maps of Australian Earthquakes, *BMR Bulletin* 214.

Gregson, P.J., and Paull, E.P., 1979 – Preliminary Report on the Cadoux Earthquake, Western Australia, 2 June1979, *Bureau of Mineral Resources, Australia, Report* 215.

Gregson, P.J., 1980 – Mundaring Geophysical Observatory Annual Report, 1979, *Bureau of Mineral Resources, Australia, Record* 1980/51

Hadzievski, D, 1976 – Seismicity on the territory of SR Macedonia, *Publication of the Seismological Observatory at the University "St. Kiril and Metodij"*, Skopje, 1976.

Kárnik, V., 1969 – Seismicity of the European area, *Csechoslovak Academy of Science,* D.Reidel Publishing Company, Holland, 1969.

Kövesligethy, R 1907 – Seismischer starkesgard u. intensitat der beben. *Gerl. Beitr. Geophys.*, Band viii, Leipzig.

Lewis, J.D., Daetwyler, N.A., Bunting, J.A., and Moncrieff, J.S., 1981 – The Cadoux earthquake, 2 June 1979, Geological *Survey of Western Australia, Report* 11.

M^{c}Cue, K.F., Dent, V., and Jones, T., 1995 – The characteristics of Australian strong ground motion, *Proceedings of the Pacific Conference of Earthquake Engineering,* Melbourne, November 1995.

Zátopek A., 1968 – The Skopje earthquake 1963, *Report of the UNESCO Technical Assistance Mission,* Amsterdam, 1968.

LESSONS FROM ALTERNATIVE ARRAY DESIGN USED FOR HIGHFREQUENCY MICROTREMOR ARRAY STUDIES

MICHAEL W. ASTEN
MONASH UNIVERSITY

AUTHOR:

Michael Asten is a Principal Research Fellow at Monash University part-time, and is also a consulting geophysicist and Partner with Flagstaff Geo-Consultants, Melbourne. He majored in Physics, Geology and Geophysics at the University of Tasmania, and gained a PhD in geophysics from Macquarie University on the topic of using microseismic waves as a tool for studying sedimentary basins. In 1977 he took up a two-year appointment lecturing and coordinating an MSc (geophysics) programme in Nigeria. He then joined BHP Minerals in 1979 and worked in coal and base-metal exploration in Australia, East Africa and North America, with particular emphasis on geophysical research issues. He initiated a numerical modelling project in in-seam (coal) seismic modelling which became a standard tool in interpretation of commercial surveys. In the last decade he has specialised in electromagnetic and gravity exploration methodologies for mineral exploration, and is author or co-author of 79 technical papers. He is collaborating with Geoscience Australia, University of Melbourne, and the US Geological Survey in the development of passive seismic methods for geotechnical and site classification tasks. He was a co-recipient of the CSIRO Medal for External Research in 2000 and co-recipient of the ASEG Graham Sands Award in 2001, (both of these for development of the "Falcon" airborne gravity gradiometer).

Email: masten@mail.earth.monash.edu.au

ABSTRACT:

Array observations of the high-frequency microtremor wave field are a useful tool for gaining thickness and low-strain shear strength of sediments for purposes of earthquake hazard site classification. The spatial autocorrelation (SPAC) method of processing data is effective in yielding wave velocity data from multi- and omni-directional sources. A model study of single pair, triangular, hexagonal and square arrays shows that the triangular or hexagonal arrays provide adequate azimuthal averaging for application of the SPAC method to studies of microtremors, provided the plane-wave sources have an azimuthal spread of order 60°. Plots of the imaginary part of the averaged coherency provide an additional indicator of quality of the averaging, with the hexagonal array having a further advantage that the imaginary part is zero for all frequencies for noise-free data, and hence deviations from zero provide a measure of statistical noise in the coherency estimates. The use of single pairs of geophones, square or linear cross arrays requires that sources have an azimuthal spread exceeding 90°, and, even with such a spread of sources, such arrays may yield averaged coherencies which deviate strongly and variably from the ideal J_0 curve. Routine plotting of the imaginary part of the averaged complex coherency provides a useful quality control on SPAC methods.

Paper No. 14

1. INTRODUCTION

The use of small seismic arrays for velocity studies of microtremors is gaining in popularity. Microtremor wave energy as detected by vertical-component geophones consists predominantly of fundamental-mode surface waves of the Rayleigh type. If the dispersion curve of phase velocity vs frequency can be measured with an array, then the shear-velocity profile of the earth local to the array can be established by iterative curve-fitting or inversion methods. A companion paper by Asten et al (2003) provides an overview of relevant literature and examples. Okada (2003) and Tokimatsu (1997) provide detailed reviews.

The most successful results from array studies of high-frequency microtremors (> 1Hz) have been achieved using the spatial autocorrelation method (SPAC) first described by Aki (1957), also called the method of spatially averaged coherencies. The strength of SPAC techniques is that they are effective in yielding wave scalar velocity when the wave field is multi-directional or omni-directional, whereas beam-forming methods (eg Capon, 1969; Liu et al, 2000) lose resolution when multiple sources are present.

In this paper we study three array types in order to develop criteria for adequacy of the spatial averaging process, and to recognise features of field data which indicate when assumptions of spatial averaging have been violated with adverse effects on accuracy of phase velocity estimates.

2. ARRAY TYPES USED IN HIGH-FREQUENCY MICROTREMOR OBSERVATIONS

The classic array shapes reported in literature are triangular three or four-station arrays shown in Figure 1 (a-b). Asten (1976, 2001), Asten et al (2002) and Asten et al (2003) use a seven-station hexagonal array (Figure 1c) in order to improve spatial averaging and provide measurements over multiple inter-station separations. More dense arrays of up to 36 stations in a semi-circular geometry have been used by Chouet et al (1998, and references therein) for study of surface-wave propagation near volcanoes, but this sophistication of design is rarely possible in microtremor surveys intended to cover multiple sites. Ohori et al (2002) used a linear cross array which can be approximated for the purpose of this study as a five-station square array (Figure 1d).

3. MODELLING SPAC

The process of modelling SPAC for an azimuthal distribution of noise-free plane waves, as observed by a set of geophone pairs distributed in azimuth, may be expressed as a summation of complex coherencies c (f) of amplitude unity, and phase given by

$$c(f) = exp\ \{\ i\, rk\, cos(\theta - \phi)\ \},$$

where r is the displacement of one geophone relative to a reference geophone, at azimuthal angle θ, k is the spatial wavenumber at frequency f, and ϕ is the azimuth of propagation of the plane wave across the array.

In the ideal case of a single plane wave observed by an infinity of geophones placed around a circle centred on a single reference geophone, the summation is expressed as an integration which yields a purely real SPAC, given by Okada (2003, equ. 3.72) as

$$\frac{1}{2\pi}\int_0^{2\pi} \exp\{irk\cos(\theta-\phi)\}d\theta = J_0(rk) \qquad -(1)$$

where J_0 is the Bessel function of the first kind of zero order with the variable rk. The same result will be obtained for omni-directional plane waves (an infinity of azimuths) observed by a single pair of geophones (ie integrate over ϕ with θ fixed).

In this study we investigate the quality of the approximation when the plane wave sources are restricted to a range of azimuths Δ (where $\Delta < 2\pi$), and a finite number of n geophones equi-spaced around the circle. For simplicity the azimuthal range is approximated in this study by a finite set of propagation directions at intervals of 1° over the range Δ. We make the strict assumption that wave energy at any frequency propagates at a single scalar velocity (commonly the fundamental Rayleigh mode for vertical-component microtremor energy). The left-hand side of equ (1) thus becomes a double summation over a finite number of plane waves, and n geophone pairs. The averaged coherency is in general a complex number, hence we compare both the real and imaginary parts of the summation with the theoretical ideal of the function J_0. We also assume for the purpose of simplicity in modelling that the scalar wave velocity is constant with respect to frequency; this assumption in not true in practice, but it does not affect the SPAC method or the conclusions of this study since SPAC averaging is applied to each frequency-wavenumber independently.

Figure 2 (a-d) shows the modelled SPAC for a relatively narrow band of wave directions ($\Delta = 30^\circ$), for a single geophone pair. As expected the SPAC has no resemblance to J_0. However in Figure 2 (e-h) when the azimuthal spread is increased to $\Delta = 90^\circ$, *Real (c(f))* may approximate J_0, depending on the degree of symmetry of the source azimuth with respect to the geophones.

Figure 3 (a-d) shows the modelled SPAC for a relatively narrow band of wave directions ($\Delta = 30^\circ$), for a triangular geophone array. Depending on the degree of symmetry of the source azimuth with respect to the geophones, *Real (c(f))* may approximate the ideal J_0 (as in (a) and (c)). However for different dominant wave azimuths, *Real (c(f))* may also depart severely from the ideal J_0. The imaginary part of the finite summation *Im (c(f))* is in general non-zero.

When the azimuthal spread of the plane-wave field is increased to $\Delta = 60^\circ$, *Real (c(f))* approximates J_0, in all examples (Figure 3 (e-j)). We conclude from this example that when microtremor sources are distributed in azimuth over angles of order 60° , (with uniform amplitudes), then the classic triangular array is sufficient to allow valid application of the SPAC method. Note in these examples however that *Im (c(f))* is in general non-zero, and hence there is value in plotting *Im (c(f))* as an ancillary indicator of the quality of spatial averaging achieved.

Figure 4 shows modelled SPAC for a six-station hexagonal array, using the same source fields as for Figure 3. Due to the symmetry of the hexagonal array sampling the same azimuths as the triangular array, the modelled curves of *Real (c(f))* are identical with those of the previous figure. However the curves of *Im (c(f))* are all zero, a fact which is easily shown to be true for any circular array of any even number of equi-spaced stations. Note also that the pairs of plots in Figure 4 (a and c) and (f and h) are geometrically equivalent and hence produce identical plots. We conclude from this example that the hexagonal array does not have an intrinsic advantage in yielding superior spatial averaging of coherencies, but it does have the advantage of nulling the summation of *Im (c(f))*, which means that a plot of *Im (c(f))* on field data will be non-zero only due to statistical noise in the estimation of coherencies from finite time series data. In such a case, *Im (c(f))* can be used as a useful measure of data quality.

From Figures 3 and 4 (b) and (d) we see another useful indicator of quality of the SPAC process; when the second maximum of the coherency curve *Real (c(f))* departs significantly from the magnitude expected from the theoretical J_0 curve, then the higher-frequency maxima, minima and cross-overs are significantly shifted from the J_0 curve. In such cases, any attempt to deduce phase velocities by the SPAC method from the observed coherency curve will be flawed.

Finally we consider the effectiveness of SPAC in the case of a square array, which can for example represent the linear cross array used by Ohori et al (2002). With such an array, and more generally with the extended SPAC (ESPAC) technique described by Ling and Okada (1993),

Okada (2003) and used by Ohori et al (2002), the necessary averaging of azimuthal information relies on omni-directional sources rather than on multiple azimuths provided by available geophone pairs. Figure 5 shows modelled SPAC for a four-station array. The curves of *Real (c(f))* are generally poor approximations to the J_0 curve, and are strongly dependent on wave direction. With directional wave energy represented by $\Delta = 30^\circ$, it is possible to obtain a curve of *Real (c(f))* in which maxima and minima are sign-reversed relative to the J_0 curve (see eg. Figure 5c), a situation which may prove misleading in attempts to interpret such data using SPAC concepts.

4. CONCLUSIONS

A model study of single pair, triangular, hexagonal and square arrays shows that the triangular or hexagonal arrays provide adequate azimuthal averaging for application of the SPAC method to studies of microtremors, provided the plane-wave sources have an azimuthal spread of order 60°. Plots of the imaginary part of the averaged coherency provide an additional indicator of quality of the averaging, with the hexagonal array having a further advantage that the imaginary part is zero for all frequencies for noise-free data, and hence deviations from zero provide a measure of statistical noise in the coherency estimates. The use of single pairs of geophones, or square or linear cross arrays, requires that sources have an azimuthal spread exceeding 90°, and, even with such a spread of sources, such arrays may yield averaged coherencies which deviate strongly and variably from the ideal J_0 curve. Routine plotting of the imaginary part of the averaged complex coherency provides a useful quality control on SPAC methods.

5. REFERENCES

Aki, K. (1957) Space and time spectra of stationary stochastic waves, with special reference to microtremors. Bull, Earthq. Res. Inst, Vol 35, pp 415-456.

Asten M.W. (1976) The use of microseisms in geophysical exploration: PhD Thesis, Macquarie University.

Asten, M.W. (2001) The Spatial Auto-Correlation Method for Phase Velocity of Microseisms – Another Method for Characterisation of Sedimentary Overburden: in Earthquake Codes in the Real World, Australian Earthquake Engineering Soc., Proceedings of the 2001 Conference, Canberra, Paper 28.

Asten, M.W., Lam, N., Gibson, G. and Wilson, J. (2002) Microtremor survey design optimised for application to site amplification and resonance modelling, *in* Total Risk Management in the Privatised Era, editted by M Griffith, D. Love, P McBean, A McDougall, B. Butler, Proceedings of Conference, Australian Earthquake Engineering Soc. , Adelaide, Paper 7.

Asten, M.W., Dhu, T., Jones, A., and Jones, T. (2003) Comparison of shear-velocities measured from microtremor array studies and SCPT data acquired for earthquake site hazard classification in the northern suburbs of Perth W.A., this volume, in "Earthquake Risk Mitigation", Proceedings of a Conference of the Australian Earthquake Engineering Soc., Melbourne, Paper 12.

Capon, J. (1969) High-resolution frequency-wavenumber spectrum analysis. Proc. IEEE, Vol 57, pp 1408-1418.

Chouet, B., De Luca, G., Milana, G., Dawson, P., Martini, M., and Scarpa, R. (1998) Shallow velocity structure of Stromboli Volcano, Italy, derived from small aperture array measurements of Strombolian tremor. Bull. Seism.Soc. Am. Vol. 88, pp 653-666.

Liu H, Boore D.M., Joyner W.B., Oppenheimer D.H., Warrick R.E., Zhang W, Hamilton J.C. & Brown L.T., 2000. Comparison of phase velocities from array measurements of Rayleigh waves associated with microtremor and results calculated from borehole shear-wave velocity profiles. Bull. Seism. Soc. Am. Vol. 90, pp 666-678.

Ling, S., and Okada, H. (1993) An extended use of the spatial autocorrelation method for the estimation of geological structure using microtremors. Proc. 89th Conf. SEGJ. pp 44-48 (in Japanese).

Herrmann, R.B. (2001) Computer programs in seismology - an overview of synthetic seismogram computation Version 3.1, Department of Earth and Planetary Sciences, St Louis Univ.

Ohori, M., Nobata, A., and Wakamatsu, K. (2002) A comparison of ESAC and FK methods of estimating phase velocity using arbitrarily shaped microtremor arrays. Bull. Seism. Soc. Am. Vol. 92, pp. 2323-2332.

Okada, H. (2003) The Microseismic Survey Method: Society of Exploration Geophysicists of Japan. Translated by Koya Suto, Geophysical Monograph Series No. 12, Society of Exploration Geophysicists, Tulsa.

Satoh, T., Kawase, H.,Iwata, T., Higashi, S., Sato, T., Irikura, K., and Huang, H. (2001) S-wave velocity structure of the Taichung basin, Taiwan, estimated from array and single-station records of microtremors. Bull. Seism. Soc. Am. Vol. 91, pp. 1267-1282.

Tokimatsu, K. (1997) Geotechnical site characterization using surface waves, *in* Earthquake Geotechnical Engineering, editted by Ishihara. Balkema, Rotterdam.

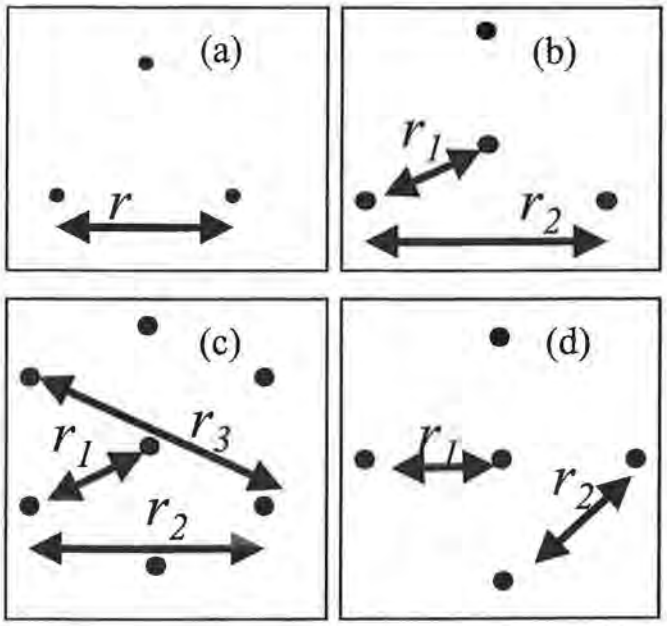

Fig. 1. (LEFT) Common array geometries used for microtremor studies using SPAC methods.

(a),(b): triangular arrays.

(c): hexagonal array. (d): square or linear cross array.

Fig. 2. BELOW. (a-d): Modelled SPAC for n=1, Δ =30°, for four different dominant directions of wave propagation. The solid line is *Real (c(f))*, dashed line is *Im (c(f))*, and the thin solid line is theoretical *Jo(kr)*. At the top right of each plot is a diagram of the array geometry (centre plus one geophone only in this case) together with an arc depicting the range of wave azimuths summed in the model.

(e-h): As for (a-d) but with azimuthal spread of wave propagation increased to Δ =90°. In (e) and (h), the plot of *Real (c(f))* closely overlays the plot of the theoretical *Jo(kr)*.

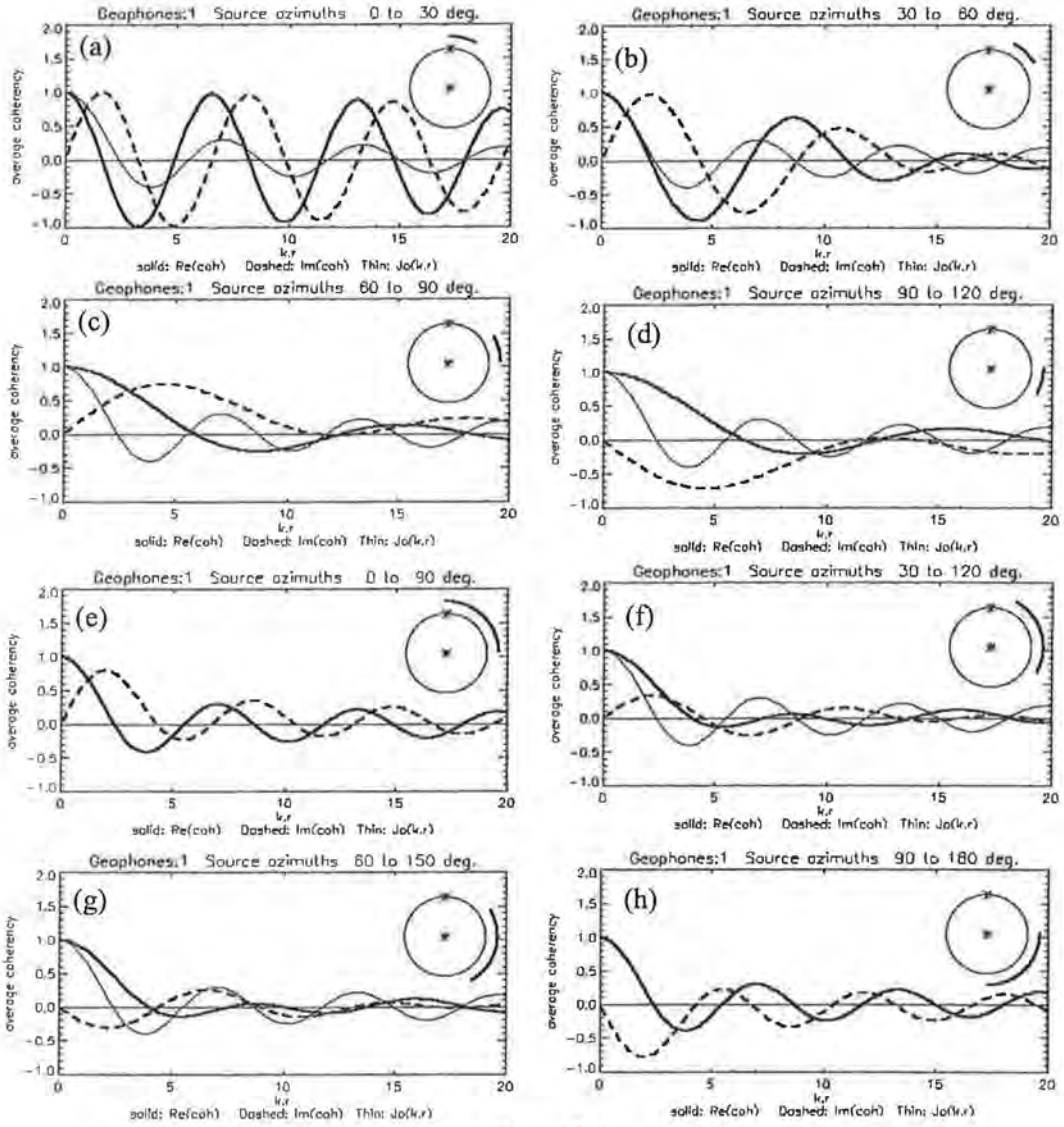

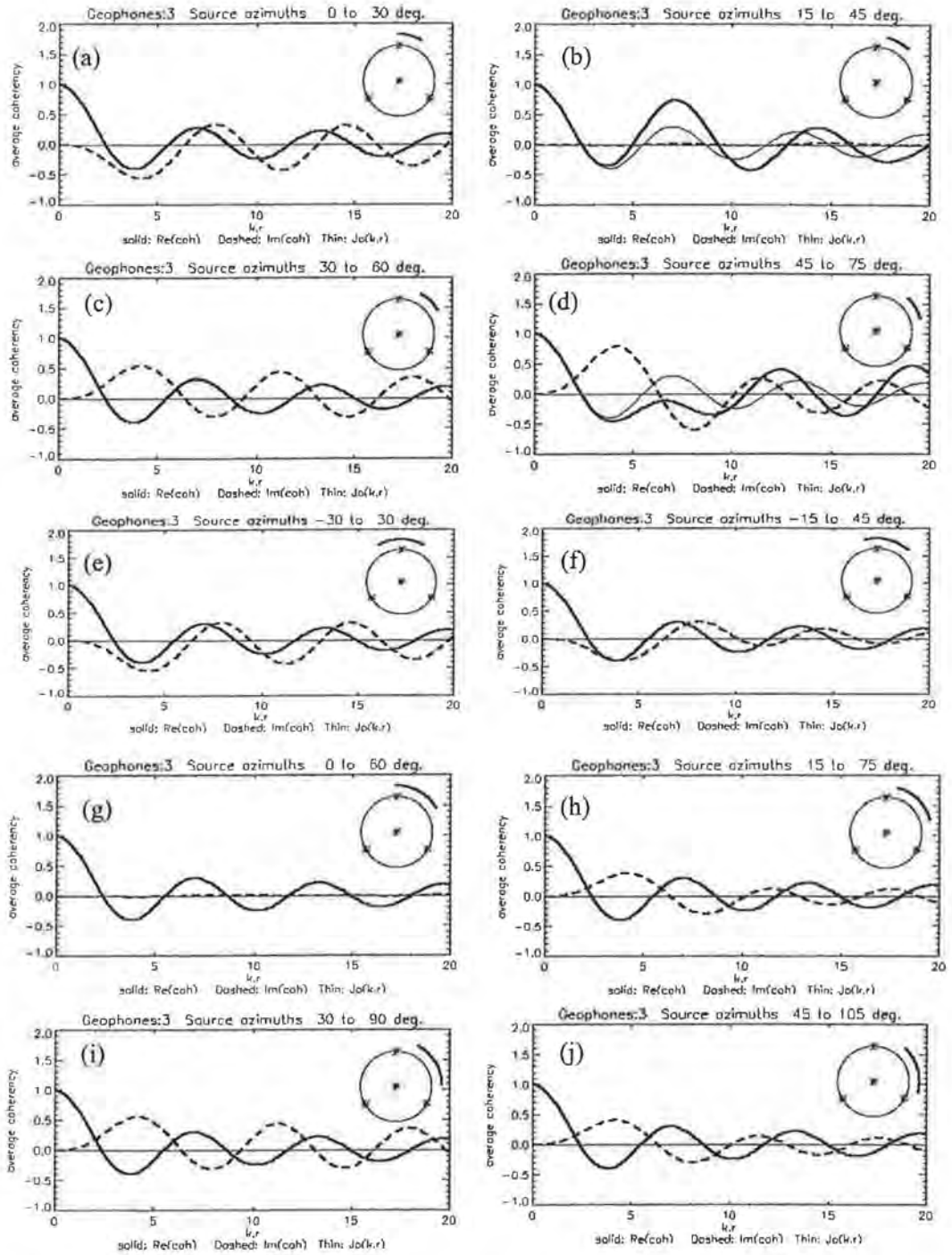

Fig. 3. (a-d): Modelled SPAC for n=3, Δ =30°, for four different dominant directions of wave propagation. The solid line is *Real (c(f))*, dashed line is *Im (c(f))*, and the thin solid line is theoretical *Jo(kr)*. At the top right of each plot is a diagram of the array geometry, together with an arc depicting the range of wave azimuths summed in the model.

(e-j): As for (a-d) but with azimuthal spread of wave propagation increased to Δ =60°. In all cases here, *Real (c(f))* ≃ *Jo(kr)*. Models (h) and (j) are geometrically equivalent and hence give the same result.

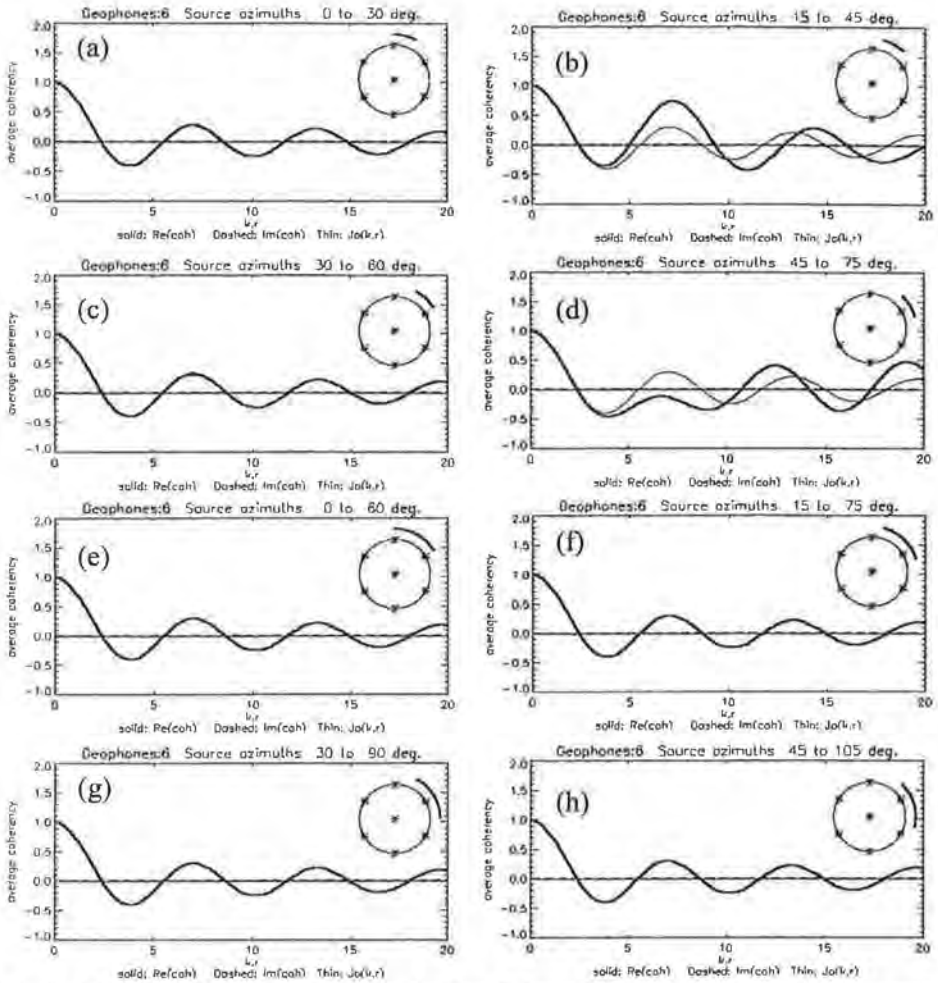

Fig. 4. (a-d): Modelled SPAC for n=3, Δ =30°, for four different dominant directions of wave propagation. The solid line is *Real (c(f))*. (The dashed line is *Im (c(f))*, all= zero in these examples). The thin solid line is theoretical *Jo(kr)*. At the top right of each plot is a diagram of the array geometry, together with an arc depicting the range of wave azimuths summed in the model. (e-h): As for (a-d) but with azimuthal spread of wave propagation increased to Δ =60°. In all cases here, *Real (c(f))* $\simeq$ *Jo(kr)*.

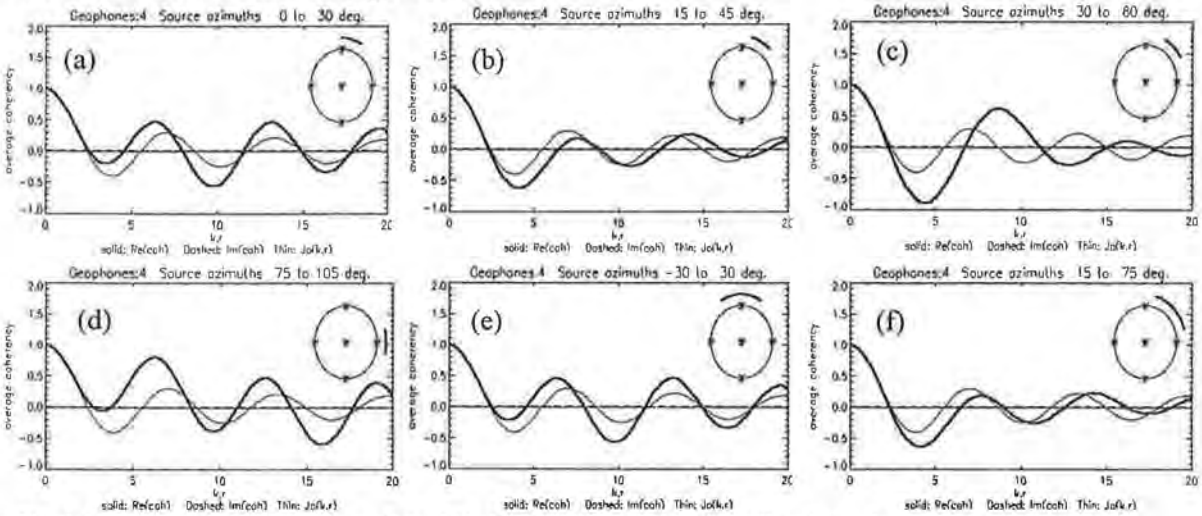

Fig. 5. (a-d): Modelled SPAC for n=4, Δ =30°, for four different dominant directions of wave propagation. The solid line is *Real (c(f))*. (The dashed line is *Im (c(f))*, all= zero in these examples). The thin solid line is theoretical *Jo(kr)*. At the top right of each plot is a diagram of the array geometry, together with an arc depicting the range of wave azimuths summed in the model. (e-f): As for (a-d) but with azimuthal spread of wave propagation increased to Δ =60°.

A DISPLACEMENT BASED APPROACH TO THE ANALYSIS FOR SEISMICALLY INDUCED TORSION IN BUILDINGS

ELISA LUMANTARNA, NELSON LAM AND JOHN WILSON
DEPARTMENT OF CIVIL AND ENVIRONMENTAL ENGINEERING
THE UNIVERSITY OF MELBOURNE

AUTHORS:

Elisa Lumantarna is a post-graduate student in the Department of Civil and Environmental Engineering at The University of Melbourne

Nelson Lam is Senior Lecturer in the Department of Civil and Environmental Engineering at The University of Melbourne

John Wilson is Associate Professor in the Department of Civil and Environmental Engineering at The University of Melbourne

ABSTRACT:

The provisions for the torsional response of buildings in contemporary seismic design standards have been based on extensive research investigating the seismic strength and ductility demand of individual lateral resisting elements in buildings with torsionally unbalanced properties. The accuracy with which the element ductility demand is estimated depends essentially on the accuracy with which the element force-displacement behaviour has been modeled. According to research in recent years into the behaviour of reinforced concrete, the yield displacement of the element estimated by conventional methods employing notional EI values could be in significant error depending on the element dimensions. These modeling uncertainties could result in the actual element strength and ductility demand to be mis-represented by observations from case studies that were reported in the literature. Consequently, there are instances in which findings from research on inelastic torsional actions appear to be contradictory.

Actions on elements expressed directly in terms of displacement are unambiguous and easier to interpret than ductility ratios. Thus, seismically induced torsional effects should be better characterized by the instantaneous centers for horizontal rotation along with the displacement of the building at its center of mass (CM). In this paper, a new torsion model employing such displacement-based parameters is introduced. With this new modeling approach, the capacity spectrum method could be extended conveniently to address inelastic torsional actions in buildings.

Paper No. 15

1. INTRODUCTION

The seismic strength demand on lateral load resisting elements in asymmetrical buildings is controlled partly by the design eccentricities which are based on implicit assumptions in the ductility behaviour of the element. The predicted ductility demand could be in error if unrealistic assumptions have been made of the element displacement at yield. For example, the element yield displacement has often been assumed to be proportional to the element yield strength. Element stiffness has also been assumed to be independent of element yield strength. Problems with the accuracies in these common assumptions have been highlighted by Paulay (2001) and Priestley & Kowalsky (1998) who rightly asserted that the yield strength of a reinforced concrete element is essentially in linear proportion to the element stiffness provided that the gross dimensions of the element and the material properties are held constant.

Uncertainties with the element ductility demand could result in mis-representation of inelastic torsional actions by case studies. Consequently, conclusions reached in different studies reported in the literature appear to be contradictory due to the different modelling assumptions (eg. Tso & Ying, 1990; Chopra & Goel, 1991). The sensitivity of the analysis results to the modelling assumptions was addressed in a recent investigation by Tso & Smith (1999).

The seismic demand on elements expressed directly in terms of displacement is unambiguous and easier to interpret than ductility ratios. Thus, seismically induced torsional effects should be better characterised by the instantaneous centers for horizontal rotation along with the displacement of the building at its center of mass (CM). The use of displacement parameters to represent inelastic torsional actions allows established displacement-based procedures such as the capacity spectrum method to be extended conveniently for 3-D analyses. With the displacement parameters and the building model defined in Sections 2 and 3, results from parametric studies to model static-dynamic modifications for elastic and inelastic systems could then be presented for comparison in the rest of the paper (Sections 4 and 5).

2. DIMENSIONLESS PARAMETERS

The dimensionless parameters associated with the new torsion model that could be adapted to the capacity spectrum method are namely α, λ and $\in$. First, the α parameter is defined as the ratio of the displacement at the center of mass (CM) of a torsionally unbalanced building (*TUB*) and the corresponding torsionally balanced building (*TB*). Thus,

$$\alpha = \frac{\Delta_{CM}\ (TUB\ )}{\Delta_{CM}\ (TB\ )} \qquad (1)$$

where Δ_{CM} (*TUB*) and Δ_{CM} (*TB*) are the displacements at the CM of a torsionally unbalanced and torsionally balanced buildings respectively.

With the displacement at the centre of mass (CM) defined by α, the maximum displacement of the torsionally responding building can be constructed "on plan" using

the λ parameter which defines the position of the instantaneous centre of rotation (ICR) of the building as shown in Figure 1b. The curve annotated as "DRE" is the envelope of the maximum displacement demand experienced at different positions in a TUB. The λ parameter has been made dimensionless by normalizing it with respect to the radius of gyration (r) of the building.

A unique solution for λ could be obtained by introducing an inertia force at the building CM in a static analysis. The rotation resulting from the inertia force causes elements on the "flexible" side of the building to experience the highest displacement demand. Displacement demand on the same elements (and the corresponding λ parameter) could then be re-evaluated by dynamic analyses employing earthquake accelerograms. The effect of dynamic torsional coupling becomes evident when the positions of the ICR, as represented by the λ parameters associated with static and dynamic actions, (denoted herein as λ_{static} and $\lambda_{dynamic}$ respectively) are compared. This static-dynamic amplification effect can be expressed conveniently by the ratio $\lambda_{dynamic} / \lambda_{static}$.

It is as important to note that static analysis shows the building rotating only in one direction (which is defined herein as the "primary rotation"). In contrast, dynamic analysis shows the building responding in both "primary" and "secondary" rotations which are represented by the dual parameters, $\lambda_{primary}$ and $\lambda_{secondary}$, as shown in Figure 1c. Thus, static analysis for torsional actions can be described as "biased" since only primary rotation has been modelled. Consequently, the displacement demand experienced by elements positioned on the "stiff" side of the building are understated by the analysis.

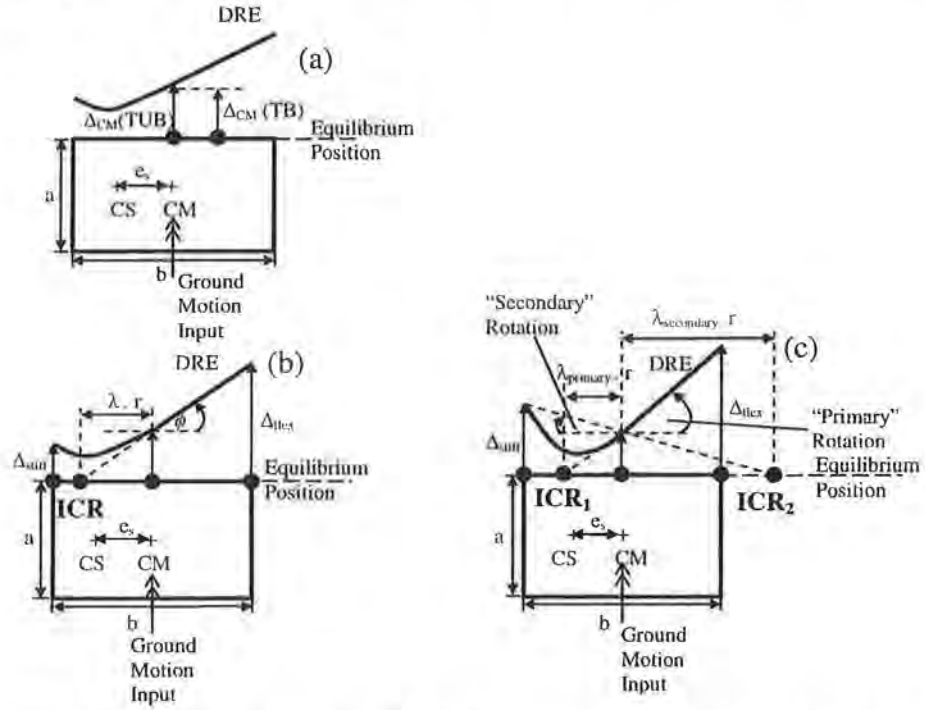

Figure 1. Definition diagrams, (a) Displacement at CM (α parameter), (b) Instantaneous centre of rotation (λ parameter), (c) "Primary" and "secondary" rotations ($\in$ parameter).

The dimensionless parameter ϵ is defined as the difference between the primary rotation ($\phi_{primary}$) and the secondary rotation ($\phi_{secondary}$) divided by $\phi_{primary}$ as shown in equation 2a. This equation can also be expressed in terms of the parameter λ as shown in equation 2b.

$$\epsilon = \frac{\left(\phi_{primary} - \phi_{secondary}\right)}{\phi_{primary}} \tag{2a}$$

$$\epsilon = 1 - \frac{\lambda_{primary}}{\lambda_{secondary}} \tag{2b}$$

The value of ϵ as defined by equation 2 varies from zero to two, with $\epsilon = 0.0$ representing static conditions in which the building responds only in primary rotation, and $\epsilon = 2.0$ representing conditions in which the primary and secondary rotations are of equal magnitude.

Displacement demand on elements resulted from elastic and inelastic torsional actions will be presented in terms of α, λ_{static}, $\lambda_{dynamic}$ and ϵ (with $\lambda_{dynamic}$ taken by default as $\lambda_{primary}$) in the rest of the paper.

3. MODELLING CONSIDERATION

Parametric studies reported in this paper were based on static and dynamic analyses of a single-storey building subject to uni-lateral excitations as shown in Figure 2. The floor plan of building shows a uni-axial eccentricity and an aspect ratio (b/a) equal to 2.5. The CM of the building is positioned at the centre of the floor plan due to the uniformity in the distribution of mass. All lateral load resisting elements incorporated into the modelling were assumed to possess a bi-linear hysteretic behaviour with a post-yield stiffness equal to 3 percent of the initial elastic stiffness. The torsional properties are represented by the two dimensionless parameters: e (the eccentricity ratio) and ρ_k (the uncoupled natural period ratio of translation to torsion) both of which have been normalised with respect to the mass radius of gyration of the building (r).

The lateral load resisting elements were designed in accordance with AS1170.4 (1993) with an acceleration coefficient of 0.15g, a site factor of 1.0, 1.5 or 2.0, and structural response factor (R_f) of 3. The building period ranges between 0.2 and 1.2 seconds. The element stiffness and strength were assumed to be in linear proportion. Consequently, the centre of strength (CV) and the centre of stiffness (CS) are coincident in position.

An ensemble of 13 recorded and synthetic accelerograms possessing a range of frequency properties were employed for the analyses (see Table 1 for details). The intensity of each record has been scaled to a PGV in the range 50-100mm/sec to represent seismic conditions for Australia corresponding to a return period of 500-2500 years. The excitations imposed an average ductility demand of about 2 on the lateral load resisting elements.

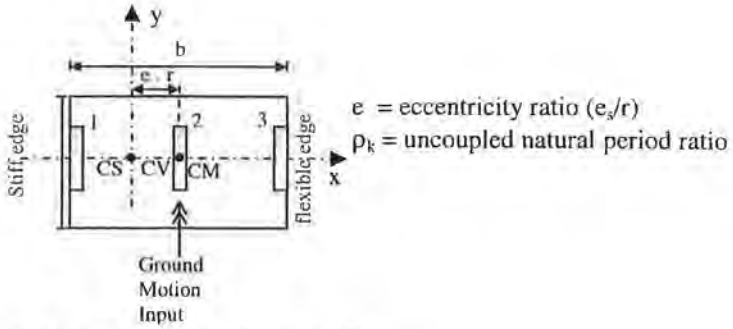

Figure 2. Plan view of the building model.

Table 1. Accelerogram ensemble employed in study.

Corner Period (T_1) (sec)	Earthquake	Direction	Magnitude	Soil
0.1 – 0.3	Parkfield, 1966	E-W	5.6	Stiff
	Friuli, 1976	Trans.	6.4	Rock
	Patras, 1974	Trans.	4.1	Rock
	Ancona-Rocca, 1972	N-S	-	Stiff
0.4 – 0.7	El Centro, 1940	N-S	6.6	Stiff
	Thessaloniki, 1978	Horz. A	5.1	Intermediate
	Gazli, 1976	N-S	7.3	Intermediate
	Leukas, 1973	Long.	5.7	Intermediate
	Kobe, 1995	N-S	6.9	Stiff
	Northridge, 1994	E-W	6.6	Stiff
>1.0	Romanian, 1977	N-S	7.2	Soft
	Synthetic (AS1170.4)	-	-	S = 1
	Synthetic (AS1170.4)	-	-	S = 2

4. ELASTIC STATIC-DYNAMIC AMPLIFICATION

4.1 Parametric studies on α

The displacement demand at the CM of the TUB and TB was analysed for the α ratio which was found to vary between 0.9 and 1.0 for the whole range of modelling parameters (see Figure 3). Thus, the displacement demand at the CM of a TUB could be estimated directly from the analysis of a single-degree-of-freedom system.

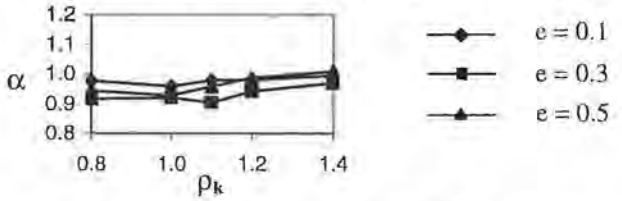

Figure 3. Median values of α parameter from dynamic analyses.

4.2 Parametric studies on λ

The displacement demand at the "flexible" edge of the building associated with primary rotation was studied next. Results from static and dynamic analyses were represented by the λ_{static} and $\lambda_{dynamic}$ parameters respectively. The values of these parameters and their

ratio $\lambda_{dynamic}/\lambda_{static}$ are presented in Figure 4a and 4b with varying values of ρ_k. A torsionally flexible building (for example, walls orientated in one direction only) will have a low value of ρ_k. It is shown in Figure 4b that increasing the torsional stiffness would result in a higher dynamic amplification of the torsional response (since a smaller ratio of $\lambda_{dynamic}$ / λ_{static} indicates a higher static-dynamic amplification). Consequently, the benefits derived from the torsional stiffness are offset partially by the dynamic amplification of the torsional rotation. Similar trends in dynamic amplification have been reported in the literature in terms of the primary effective eccentricity (Chandler & Hutchinson, 1988) which was defined as the distance from the CM of the building at which the static force is applied in order that the maximum displacement from the static and dynamic analyses matches.

Figure 4. Comparison of λ values from static and dynamic analysis for building models with e = 0.3, ρ_k = 0.8 - 1.4, (a) λ_{static} versus $\lambda_{dynamic}$, (b) Ratio of $\lambda_{dynamic}/\lambda_{static}$.

4.3. Parametric studies in ϵ

As stated earlier in the paper, the ratio $\lambda_{dynamic}$ / λ_{static} only represents the effects of primary rotation which causes elements positioned on the "flexible" side of the building to experience high displacement demand. In contrast, the ϵ parameter was introduced to account for the displacement demand experienced by elements positioned on the "stiff" side of the building. It is shown in Figure 5 that the value of ϵ decreases with increasing value of ρ_k. Thus, for a torsionally flexible building (ie. with low of ρ_k), the ϵ value approaches 2.0 implying that the secondary rotation is in the order of the primary rotation, hence elements on both the "flexible" side and the "stiff" side will be subject to comparable displacement demand. Thus, increasing the torsional stiffness has the desirable effect of suppressing such dynamic phenomenon. Similar trends have been observed in an earlier study in which negative secondary effective eccentricity was used to represent the displacement demand of elements on the "stiff" side of the building. The secondary effective eccentricity was found to be less onerous with high ρ_k values (Chandler and Hutchinson, 1988).

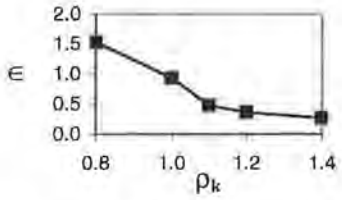

Figure 5. Median values of ϵ parameter from dynamic analysis, e = 0.3, ρ_k = 0.8 - 1.4.

5. EFFECTS OF DUCTILE YIELDING

The effect that ductile yielding has upon the dynamic torsional response behaviour of buildings has been the subject of intensive research over two decades. In this section, the sensitivity of the dimensionless parameters (α, λ and $\in$) to changes in the ductility ratio, from $\mu = 1$ (elastic behaviour) to $\mu = 2$ (limited ductile behaviour), were studied.

The value of α was found to be insensitive to the ductility ratio. Thus, limited ductile behaviour was found to have insignificant effect on the displacement of the building at the CM.

The behaviour of the other parameters namely $\lambda_{dynamic}$, the ratio $\lambda_{dynamic}$ / λ_{static}, and $\in$ have also been studied. It is shown in Figure 6a that primary rotation resulting from torsional actions could be amplified by ductile yielding particularly for buildings possessing high values of ρ_k. However, the effects of ductile yielding could be overstated by a quasi-static analysis which is an interesting contrast to the dynamic amplification behaviour that has been identified with the elastic response. The $\lambda_{dynamic}$ / λ_{static} ratio associated with elastic and inelastic behaviour are shown in Figure 6b to reveal this trend (note, a lower ratio infers a higher amplification). It is inferred from the comparison that recent studies by Paulay (1997) based on quasi-static simulations could have overstated the effects of inelastic torsional actions in buildings.

Favourable trends associated with ductile yielding were also observed with the $\in$ parameter which represents the effects of secondary rotation. The mitigating effects of ductile yielding on "secondary" rotation as shown in Figure 6c contradict the conclusions reached by Chandler and Duan (1997) in which the accentuation of secondary rotation by ductile yielding was highlighted. The high ductility demand observed from this latter study is considered by the author to be the result of very low yield strength (hence very low yield displacement) being assigned to elements positioned on the "stiff" side of the building. This comparison demonstrates the need for extreme caution in interpreting results reported in the literature.

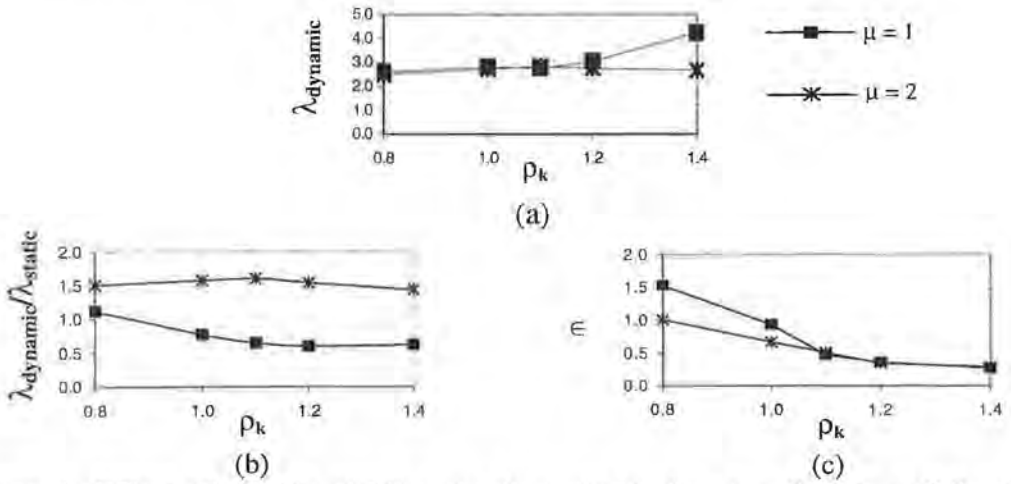

Figure 6. Effect of ductile yielding on dynamic torsion, e = 0.3, ρ_k = 0.8 - 1.4, (a) Median values of $\lambda_{dynamic}$, (b) Ratio of $\lambda_{dynamic}/\lambda_{static}$, (c) Median values of $\in$ parameter.

6. CLOSING REMARKS

A new model is introduced in this paper to address the effects of elastic and inelastic torsional actions in buildings using dimensionless parameters. This new model could be used to enhance the displacement-based methodology which was primarily developed for pure translation response, such as in the capacity spectrum method.

Using this new model, limited analyses were carried out for comparison with previous studies reported in the literature. The trends observed in this study and in previous studies with elastic responses are generally consistent. However, certain trends observed with inelastic response contradict observations previously reported in the literature.

7. REFERENCES

Standard Association of Australia (1993) Minimum Design Loads on Structures: Part 4: Earthquake Loads.

Chandler, A. M., Duan, X. N. (1991) Evaluation of Factors Influencing the Inelastic Seismic Performance of Torsionally Asymmetric Buildings, Earthquake Engineering and Structural Dynamics 20, pp. 87-95.

Chandler, A. M., Duan, X. N. (1997) Performance of Asymmetric Code-Designed Buildings for Serviceability and Ultimate Limit States, Earthquake Engineering and Structural Dynamics 26, pp. 717-735.

Chandler, A. M., Hutchinson, G. M. (1988) Evaluation of the Secondary Torsional Design Provisions of Earthquake Building Codes, Proceedings of Institution of Civil Engineers, part 2, pp. 587-607.

Chandler, A. M., Hutchinson, G. M. (1988) A Modified Approach to Earthquake Resistant Design of Torsionally Coupled Buildings, Bulletin of the New Zealand Society of Earthquake Engineering 21(2), 1988, pp. 140-152.

Chopra, A. K., Goel, R. K. (1991) Evaluation of Torsional Provisions in Seismic Codes, Journal of Structural Engineering ASCE 117(2), pp. 3762-3782.

Paulay, T. (1997) A Review of Code Provisions for Torsional Seismic Effects in Buildings, Bulletin of the New Zealand Society of Earthquake Engineering 30(3), pp. 252-263.

Paulay, T. (2001) Some Design Principles Relevant to Torsional Phenomena in Ductile Buildings, Journal of Structural Engineering ASCE 5(3), pp. 273-308.

Priestley, M. J. N., Kowalsky, M. J. (1998) Aspects of Drift and Ductility Capacity of Rectangular Cantilever Structural Walls, Bulletin of the New Zealand Society of Earthquake Engineering 31(2), pp. 75-85.

Tso, W. K., Smith, R. S. H. (1999) Re-evaluation of Seismic Torsional Provisions, Earthquake Engineering and Structural Dynamics 28, pp. 899-917.

Tso, W. K., Ying, H. (1990) Additional Seismic Inelastic Deformation Caused by Structural Asymmetry, Earthquake Engineering and Structural Dynamics 19, pp. 243-258.

THE EFFECT OF ROCK MOTIONS ON SOIL AMPLIFICATION FACTORS FOR AUSTRALIAN CONDITIONS

SRIKANTH VENKATESAN, TREVOR DHU, NELSON LAM AND JOHN WILSON
THE UNIVERSITY OF MELBOURNE AND GEOSCIENCE AUSTRALIA

AUTHORS:

Srikanth Venkatesan is a post-graduate student in the Department of Civil and Environmental Engineering at The University of Melbourne

Trevor Dhu is a research scientist at Geoscience Australia

Nelson Lam is senior lecturer in the Department of Civil and Environmental Engineering at The University of Melbourne

John Wilson is associate professor in the Department of Civil and Environmental Engineering at The University of Melbourne

ABSTRACT:

Rock motion intensity (level of ground motion measured on rock) is widely known to have significant effects on soil amplification factors. The objective of this paper is to emphasise the influence of both the rock motion intensity and earthquake magnitude on soil amplification factors. The sensitivity of soil amplification factors to rock motion intensity is studied using earthquake scenarios associated with a range of design peak ground velocities (PGV's) and peak ground accelerations (PGA's) specified for Australia. Earthquakes of varying magnitude were normalized to a constant PGA or PGV. Earthquakes with different magnitude have notably different amplification factors. It is observed from the analyses results that the variability in amplification factors is clearly affected by the choice of normalization parameter, i.e. PGA or PGV.

Paper No. 16

1. INTRODUCTION

The amplitude and frequency content of seismic shear waves reaching the earth's surface is dependent on site soil conditions. Provisions have been developed in major codes of practices including the International Building Code (IBC, 2000) in the USA to address this phenomenon. Code provisions are typically based on statistical analysis of instrumented ground motion records from which amplification factors have been identified for a series of pre-defined site classes. The site classification system in the IBC, for example, is based on the average shear wave velocity (SWV) in the sedimentary soil layers and the ground motion intensity. Other codes of practice such as the draft Joint Australian-New Zealand Standard (AS/NZS, 2003) have incorporated the site natural period as one of the criteria for site classification. Soil amplification is also controlled by other parameters including the SWV gradient, thickness of soft soil layers, overall soil depth, impedance contrast at the soil-rock interface, and response spectrum representing the frequency content of seismic waves measured on bedrock. The influence of these parameters on soil behaviour is generally understood by researchers, and can be demonstrated by simple one-dimensional shear wave analysis of a soil column. However, it is believed that these effects are not necessarily appreciated by the broader spectrum of practitioners in Australia.

Research is currently being undertaken by the University of Melbourne in collaboration with Geoscience Australia to develop a generalized soil amplification model that could be applied to Australia and to other intraplate regions where local ground motion data is sparse. In addressing the scarcity of data, procedures have been developed to simulate bedrock motions based on a stochastic modelling technique [Lam 2000, Chandler 2002]. One-dimensional quasi-linear analysis of soil columns is used in this study given the limited input information. The use of this simple and inexpensive methodology for soil response analysis is well supported in the literature [Dickenson 1991, Seed 1994, Dobry 2000] despite its shortcomings in modeling 3-D effects such as the basin-edge effects (Somerville, 2000).

This paper presents preliminary research findings related to the effects of motion intensity on soil amplification factors. More specifically, this paper investigates the different trends in amplification factors observed when ground motions are normalized to different ground motion intensity measures. Two soil columns were used in the study based on borehole records from Newcastle (denoted "Site-1") and from Melbourne (denoted "Site-2"). These two soil columns possess site periods of 0.5 sec and 0.9 sec respectively, and are both site class 'D' in the IBC classification system due to the presence of soft soil layers possessing very low shear wave velocity. Bedrock accelerograms have been simulated for earthquake scenarios of magnitude ranging between M5 and M8, using a stochastic procedure [program "GENQKE" (Lam, 2000)]. The pseudo non-linear site response program SHAKE-91 (Schnabel, 1972) has been used for the 1-D site response analysis of the soil columns.

2. DEFINITIONS OF MOTION INTENSITY

All response spectra of rock sites have been normalized with respect to a ground motion intensity parameter [PGA or PGV to describe the level of ground motion, not the same as traditional 'intensity'] in order that the sensitivity of the soil amplification factor to the particular parameter could be identified. The peak ground velocity PGV and the peak ground acceleration PGA are the two parameters that have been used for this normalization. In this study, PGV is taken as the maximum response spectral velocity (RSV max) divided by 1.8. Thus, response spectra that have been normalized to a common PGV of 60mm/sec have RSV_{max} equal to 110mm/sec for both the M5.5 and M7 earthquake scenarios (see Figure 1). The targeted PGV's were obtained by adjusting the hypocentral distance in each of the earthquake considered.

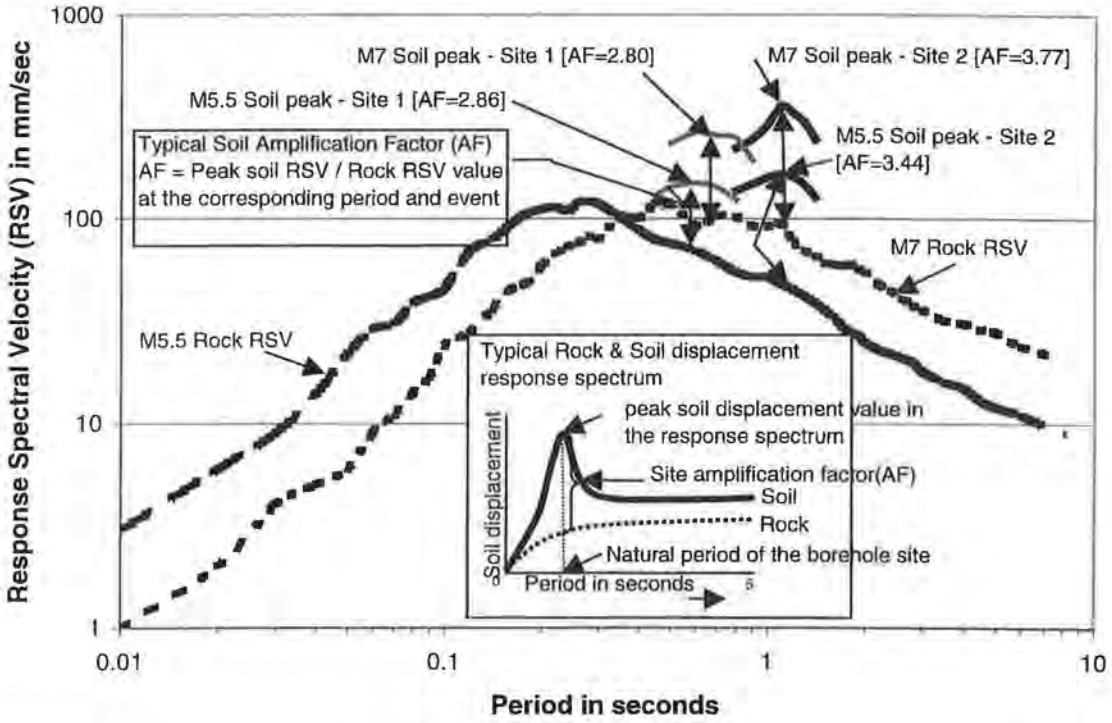

Figure 1. Analyses of soil amplification actors for sites with natural periods of 0.5 sec [Site 1] & 0.9 sec [Site 2] normalised to a PGV= 60 mm/sec

The soil response spectra representing the effects of site resonance are typified by "peaks" as shown in Figure 1. Only the part of the soil response spectrum at the resonant peak is shown in the figure (the rest of the spectrum displaying higher mode effects are not shown). The alternative displacement response spectrum format displays the fundamental resonant peak even more prominently (see inset diagram, Figure 1.). The soil amplification factor (AF) is defined herein as the maximum ratio of the soil and rock response spectrum at the resonant peak. At a PGV of 60 mm/sec, the AF's obtained from the analysis of two earthquake scenarios for the two soil columns range between 2.8 and 3.8. According to the Australian Standard AS1170.4 (1993), the acceleration coefficient (a) in g's is defined as the PGV in millimeters per second divided by 750. Thus, the AF values similar to that shown in Figure 1 should be

obtained from bedrock excitations that have been normalised to a value of a = 0.08 g or PGV of 60 mm/sec.

In order to investigate the effect of normalizing by different parameters, the ground motions used in Figure 1 were normalized to a constant PGA of 0.08 g (equivalent according to AS 1170.4 to a PGV of 60 mm/sec). These normalized ground motions were then used to calculate amplification factors for the two sites of interest (Figure 2). The AF's obtained from this analysis for the two soil columns are within the range 2.4 - 4 (compared to the range 2.8 – 3.8 at a PGV of 60 mm/sec). Interestingly, the rock response spectra and the AF's associated with the two normalization approaches are noticeably different. (compare Figure 1 with Figure 2). This suggests that the intensity parameter used for normalization might affect the AF values. This phenomenon is investigated further in the next section, which presents separate correlations of AF's with PGV and AF's with PGA.

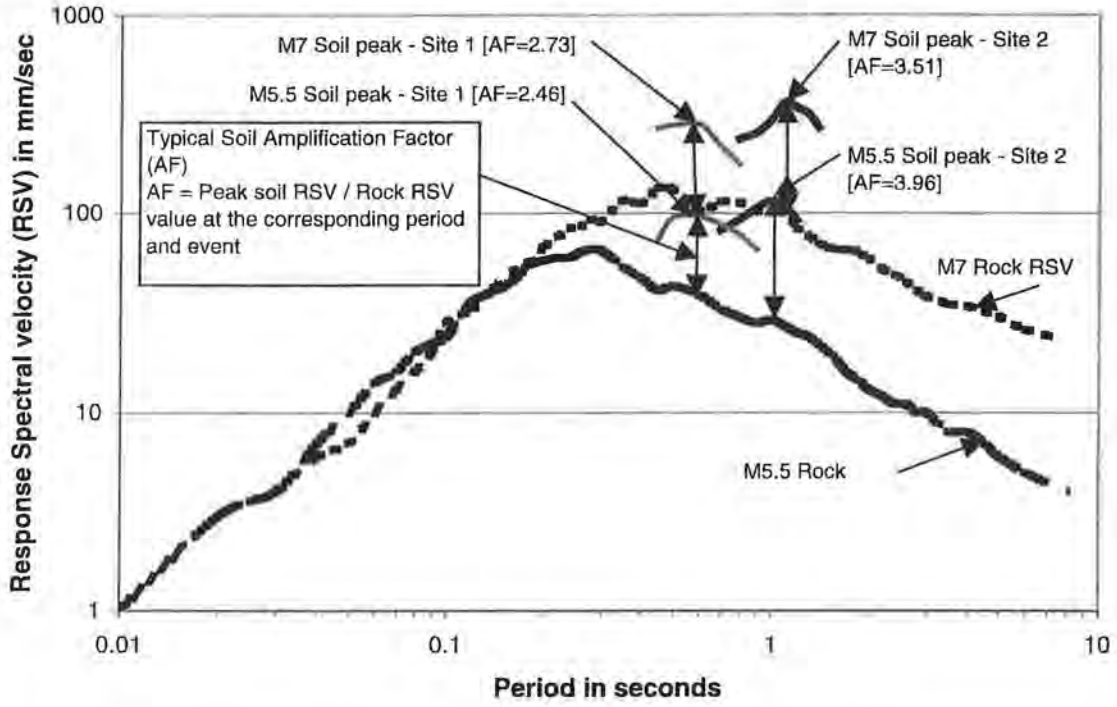

Figure 2. Analyses of soil amplification factors for sites with natural periods of 0.5 sec [Site 1] & 0.9 sec [Site 2] normalised to a PGA= 0.08g

3. INTENSITY AND MAGNITUDE EFFECTS ON SOIL AMPLIFICATION

Amplification factors were calculated for the 0.9 sec period site ("site-2") based on earthquake scenarios with PGV's varying between 20mm/sec and 100mm/sec. The overall trend of AF decreasing with increasing PGV is in agreement with the code provisions, and generally accepted in practice. However, the AF values are some 1.5 times higher than the recommendations by IBC for site Class D (Figure 3). The AF's associated with the M5.5 and M7 earthquake scenarios were very similar. In contrast, the correlations of AF with PGA are highly dependent on the earthquake magnitude (see Figure 4).

The AF-PGV and AF-PGA correlations obtained for the 0.5sec and 0.9 sec period sites are presented in Figures 5 & 6 respectively. A slightly higher amplification is observed for the 0.9 sec period site, but the difference is not large. Significantly, the correlations of AF's with PGV show much less scatter than the correlations of AF's with PGA.

Finally, the sensitivity of AF's to earthquake magnitude is presented in Figure 7 with PGV held constant at 60 mm/sec. A moderate (10-20%) increase in AF is shown with the earthquake magnitude increasing from M5.5 to M8.

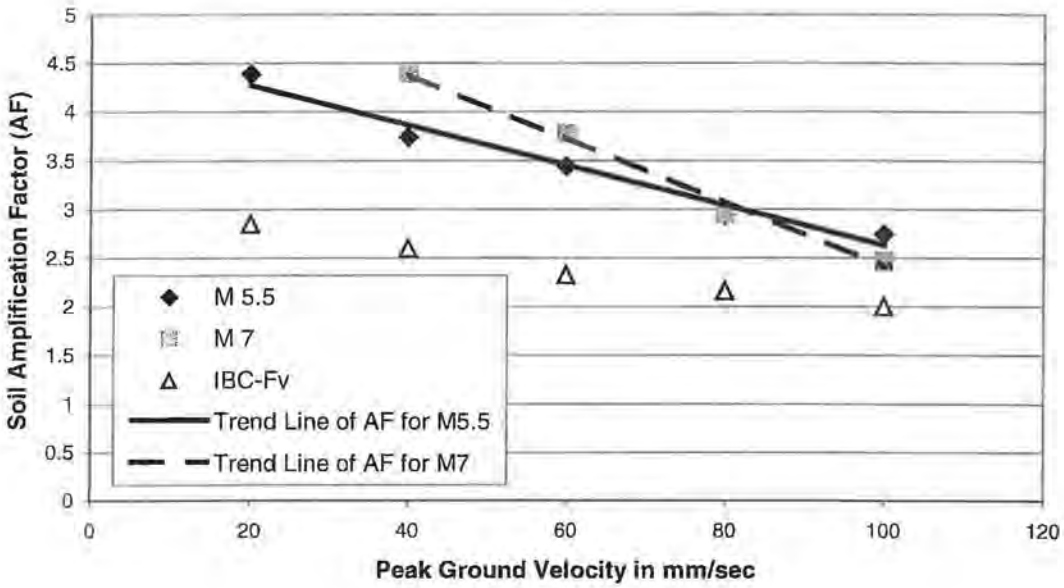

Figure 3. Soil amplification factor versus PGV for 0.9 sec site [Site-2]

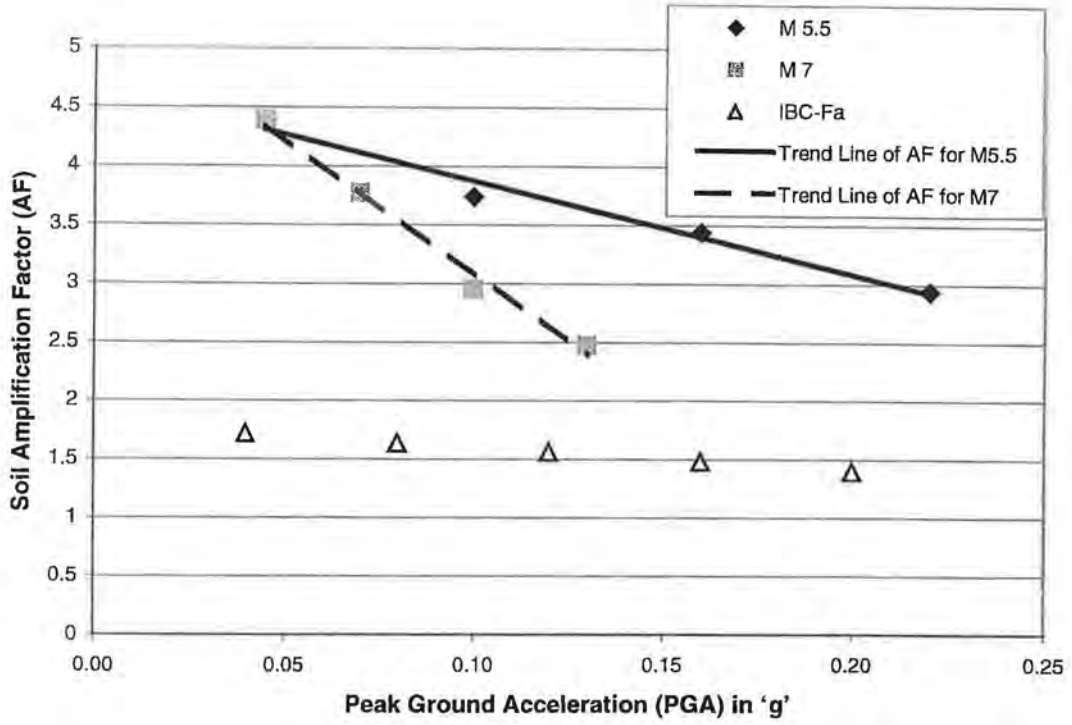

Figure 4. Soil amplification factor versus PGA for 0.9 sec site [Site-2]

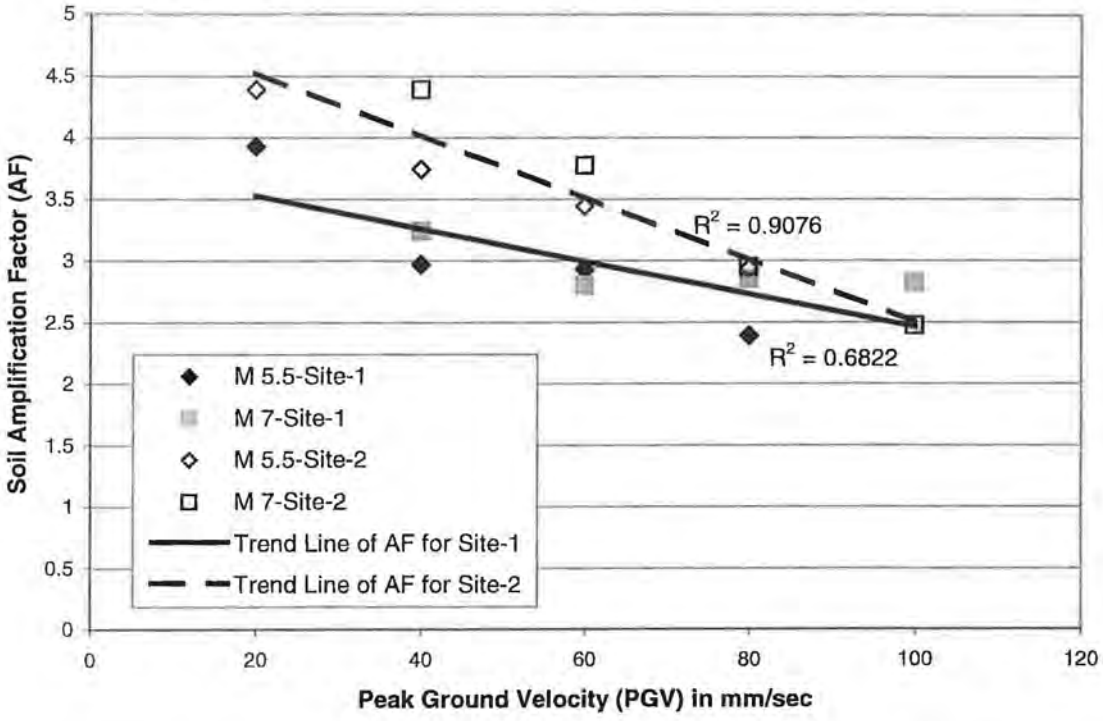

Figure 5. Influence of Magnitude and PGV on soil amplification factor

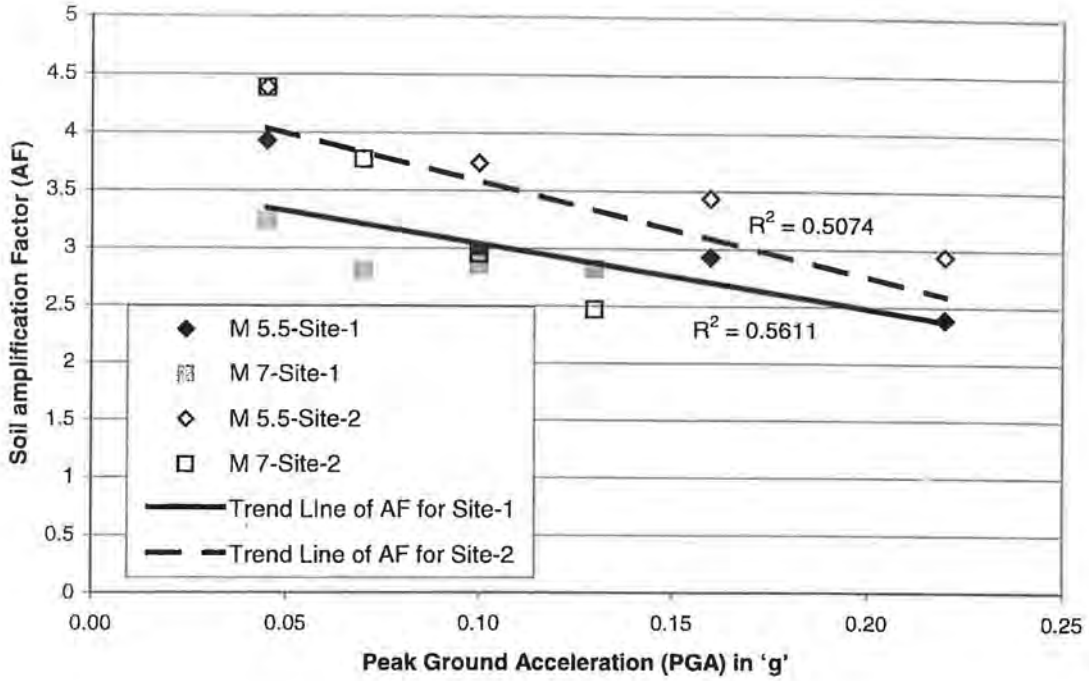

Figure 6. Influence of Magnitude and PGA on soil amplification factor

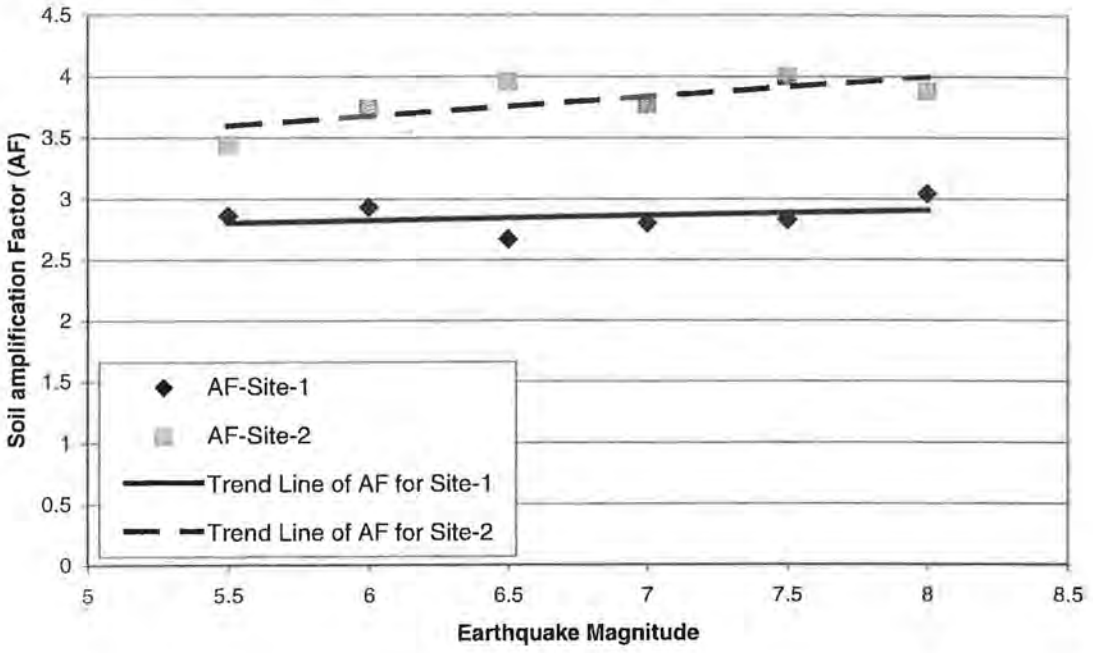

Figure 7. Influence of Magnitude on soil amplification factor with a constant PGV=60 mm/sec

4. CLOSING REMARKS

This paper emphasizes the dependence of soil amplification on earthquake magnitude, rock motion intensity, and site natural period. Importantly, the effects of the choice of normalization parameter (PGA or PGV) on AF's have been highlighted. Other trends that are well understood by researchers who regularly deal with site response issues and perhaps not fully appreciated by general practitioners have also been highlighted. Moreover, there are significant shortcomings in generalized AF's, with the AF's computed in this paper, some 1.5 times higher than the IBC code recommendations.

This paper only considered two distinct sites. Further investigation is being undertaken to obtain similar and more generalized correlations with a large number of sites. This work will lead to generalized relationships for soil amplification factors.

5. REFERENCES

Australian Standard - AS 1170.4, 1993, Minimum design loads on structures, Part 4: Earthquake loads, Standards Association of Australia, North Sydney, NSW, Australia

Chandler, A.M., Lam, N.T.K., and Sheikh, M.N., 2002, Response spectrum predictions for potential near field and far field earthquakes affecting Hong Kong: Soil sites, Journal of Soil Dynamics & Earthquake Engineering, No.22, pp. 419-440.

Dickenson, S.E., Seed, R.B., Lysmer, J., and Cok, C.M., 1991, "Response of soft soils during the 1989 Loma Preita earthquake and implications for seismic design criteria", Proceedings of the Pacific conference on earthquake engineering, New Zealand, pp 191-203.

Dobry, R., Borcherdt, R.D., Crouse, C.B., Idriss, I.M., Joyner, W.B., Martin, G.R., Power, M.S., Rinne, E.E., and Seed, R.B., 2000, New site coefficients and site classification system used in recent building seismic code provisions, Earthquake Spectra, Vol.16, No.1, pp. 41-67.

International Building Code – IBC 2000, 2000, International Code Council (ICC), USA.

Joint Australian New Zealand Standard Draft AS/NZS 1170.4 Commentary 2003, Structural Design Actions Part 4: Earthquake actions, Standards New Zealand, Wellington, New Zealand

Lam, N.T.K., Wilson, J.L., and Hutchinson G.L., 2000, Generation of synthetic earthquake accelerograms using seismological modeling: a review, Journal of Earthquake Engineering, Vol 4, No 3, pp 321-354.

Schnabel, P.B., Lysmer, J., and Seed, H.B., 1972, A computer program for earthquake response analysis of horizontally layered sites. Earthquake Engineering Research Centre EERC report 72-12. Berkeley (CA): University of California at Berkeley.

Seed, R.B., Dickenson, S.E., Rau, G.A., White, R.K., and Mok, C.M., 1994, Observations regarding seismic response analyses for soft and deep clay sites, Proceedings of the 1992 NCEER/SEAOC/BSSC Workshop on site response during earthquakes and seismic code provisions, National Centre for Earthquake Engineering Research Special Publication NCEER-94-SP 01, Buffalo, NewYork.

Somerville, P., 2000, Seismic Hazard Evaluation, 12th World Conference on Earthquake Engineering, Vol. 2, No. 2833, pp.371-385.

THE SEISMIC ASSESSMENT OF SOFT-STOREY BUILDINGS IN MELBOURNE

KITTIPOOM RODSIN, JOHN WILSON, NELSON LAM AND HELEN GOLDSWORTHY
THE UNIVERSITY OF MELBOURNE

AUTHORS:

Kittipoom Rodsin is a post-graduate student in the Department of Civil and Environmental Engineering at The University of Melbourne

Nelson Lam is a senior lecturer in the Department of Civil and Environmental Engineering at The University of Melbourne.

John Wilson is an associate professor in the Department of Civil and Environmental Engineering at The University of Melbourne.

Helen Goldsworthy is a senior lecturer in the Department of Civil and Environmental Engineering at The University of Melbourne.

ABSTRACT:

Buildings with soft-storeys are well known to be particularly vulnerable to collapse and severe damage under earthquake excitation. Despite this, buildings possessing soft-storey features are commonly found in low to moderate seismic countries such as Australia. Cost effective retrofitting of soft-storey buildings to improve seismic performance is possible if the seismic demand and building capacity can be realistically estimated. Conventional seismic design procedures involve the determination of the building's seismic base shear demand using a structural response factor to account for inelastic action and overstrength. Such methods are approximate and do not provide guidance on likely seismic performance under an extreme event.

This paper presents a simple and effective non-linear static procedure to compare the seismic demand and capacity of a soft-storey structure. The seismic demand is represented by a recently developed response spectrum model that realistically estimates the maximum acceleration, velocity and displacement response in ADRS format. The capacity of the soft-storey is ascertained using a deformation model that accounts for the effects of axial compression, flexure, shear, column-end rotation and foundation flexibility. The uneven sharing of shear forces between the columns and the significant additional shear demand associated with strut actions in masonry infill are amongst the numerous important issues that are raised for special attention. A proposed experimental program to evaluate the accuracy of the analytical procedure is described.

Paper No. 17

1. INTRODUCTION

A soft-storey possesses horizontal stiffness and/or strength properties that are much less than that of adjacent storeys and are typically the weak link in the resistance of the building to horizontal loading. The concentration of damage in the soft-storey often results in building collapse under severe seismic excitations. Soft-storey construction is commonly associated with poor seismic performance and is prohibited by regulatory controls in most high seismic regions. However, buildings featuring soft-storeys are still commonly found in regions of low or moderate seismicity including Australia. A recent survey by the authors of high-rise apartment buildings around the metropolitan area of Melbourne revealed the widespread use of reinforced concrete portal frames, which are designed to transfer vertical and horizontal loads from the first floor level to the ground floor level. The flexible portal frames which constitute a soft-storey are designed to support the "rigid-block" like upper floors consisting typically of reinforced concrete walls and slabs. This paper presents the findings from an analytical investigation into the seismic response behaviour of typical soft-storey buildings using a case study building.

The traditional force-based approach in current codes of practices uses a "structural response factor" (R_f) to account for both overstrength and inelastic response behaviour of a building structure. The complex non-linear behaviour of a soft-storey is influenced significantly by factors such as axial compression and shear span-depth ratio of the columns and cannot possibly be modeled accurately and reliably by a single R_f parameter. Furthermore, there are no specific provisions in current codes of practices (e.g. AS1170.4, 1993) to address soft-storey structures.

Non-linear static procedures (NSP) seem to be the most suitable method for assessing the seismic performance of buildings possessing soft-storey features. In this paper, results from analyses using NSP are presented in the acceleration-displacement response spectrum (ADRS) format [ATC-40, 1996] to illustrate the performance of a soft-storey building.

2. CAPACITY PREDICTION OF SOFT-STOREY BUILDINGS

The force-displacement behaviour of a typical soft-storey building is illustrated in this section using a case study example. The lateral displacement of the soft-storey primarily results from the deformation of the columns consisting of flexural deformation, shear deformation, yield penetration and end joint rotation.

Flexural deformation can be relatively accurately estimated by integrating curvatures that have been calculated in accordance with representative stress-strain relationships of both the concrete and steel [Watson et al., 1994] assuming plane section remaining plane. Shear deformation is particularly significant with short columns possessing low shear-span to depth ratios. In this study, a truss analogy method developed for cracked concrete [Park and Paulay, 1975] was used to predict shear deformation assuming linear elastic behaviour of the concrete "struts" and the steel "ties". An alternative method would be to use compression field theory [Vecchio and Collin, 1986].

The effects of yield penetration in the column longitudinal reinforcement at the anchorage to the foundation was calculated in accordance with the recommendations by Alsiwat and Saatcioglu [1992]. Finally, end rotations of the column contributed mainly by the flexibility of the piled foundation and the connecting ground beams have been incorporated into the analysis according to the recommendation in ATC-40 [1996]. The relative contributions from each of the deformation mechanisms to the total deformation of the column have been studied by push-over analysis using the example column shown in Figure 1.

The displacement behaviour of the portal frame as a whole was also studied. Analysis results show that compressive stresses in the columns arising from the "push-pull" actions associated with the application of the horizontal load could be very significant (refer Figure 2). The initial axial load ratio of 0.15 under gravity loading could be increased to 0.3 as the horizontal force is applied to the frame. Importantly, the stiffness properties of the column are very sensitive to the induced axial compression. Consequently, columns within the same portal frame possess very different stiffness properties. The force-displacement relationships (defining the effective stiffness) of the individual columns along with that representing the portal frame as a whole are presented in Figure 3 (points 1 to 3). The analytical deformation model described previously (refer Figure 1) was augmented by the empirical model of Panagiotakos and Fardis [2001] to extrapolate the response to failure. (i.e. beyond the point annotated with a "3" in Figure 3)

The differential stiffness in the columns resulted in a very uneven sharing of the horizontal shear forces between the columns within the portal frame. In the presented case study of a 13-storey building (Figure 2), the more heavily loaded column (i.e. column subjected to a higher compressive stress) attracted twice the shear force of a lightly loaded column. Such differential load-sharing between the columns is typically not modeled by the commonly used structural analysis packages. Thus, the seismically induced shear forces in soft-storey columns are often understated by conventional analyses.

Finally, the calculated displacements of the superstructure (associated with tilting of the foundation) and P-delta effects have been included in the analysis to obtain the force-displacement relationship of the whole building (refer Figure 3).

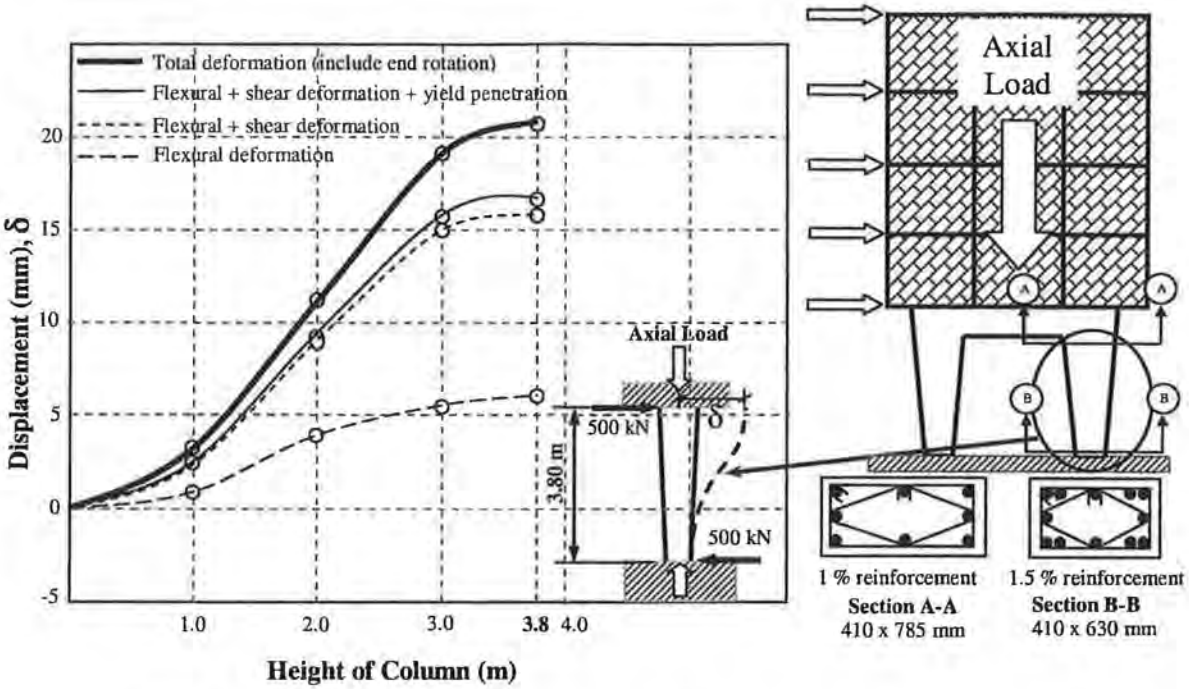

Figure 1. Deformation along the height of column subjected to horizontal shear

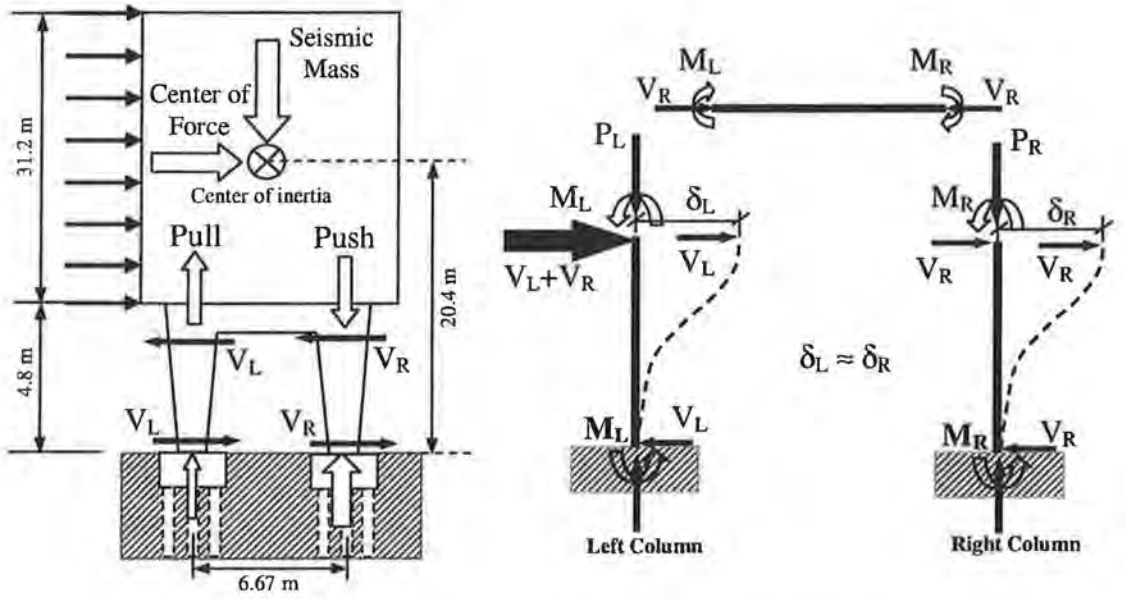

Figure 2. Portal frame under axial load variations

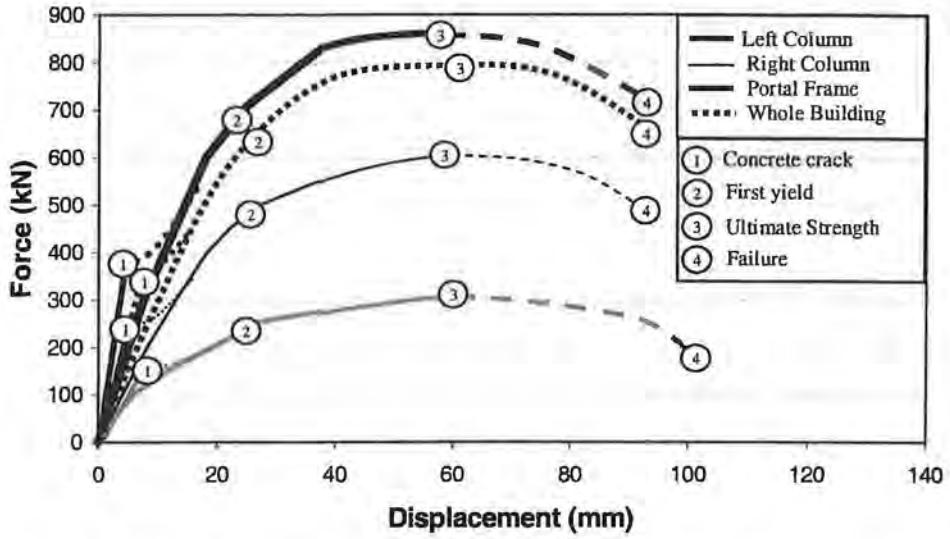

Figure 3. Shear – displacement behavior of columns, portal frame and whole building

3. PERFORMANCE EVALUATION OF SOFT-STOREY BUILDINGS

The potential seismic performance of the soft-storey building was assessed by the capacity spectrum method (CSM) [ATC-40, 1996] based on the force-displacement relationships developed in Section 2. An introduction to CSM can be found in Wilson and Lam [2003]. The assumed seismic demand was based on provisions incorporated in the draft Joint Australian/New Zealand Standard for Earthquake Actions [AS/NZS 1170.4 Draft No.8: 2003]. Information from borehole records taken from the area indicates a Class C site. The performance point obtained by intercepting the demand curves with the force-displacement (capacity) curves has displacement in the order of 20mm and the corresponding acceleration is 0.14g approximately (refer Figure 4). This may conclude that under the earthquake, this building will perform satisfactorily under the elastic limit.

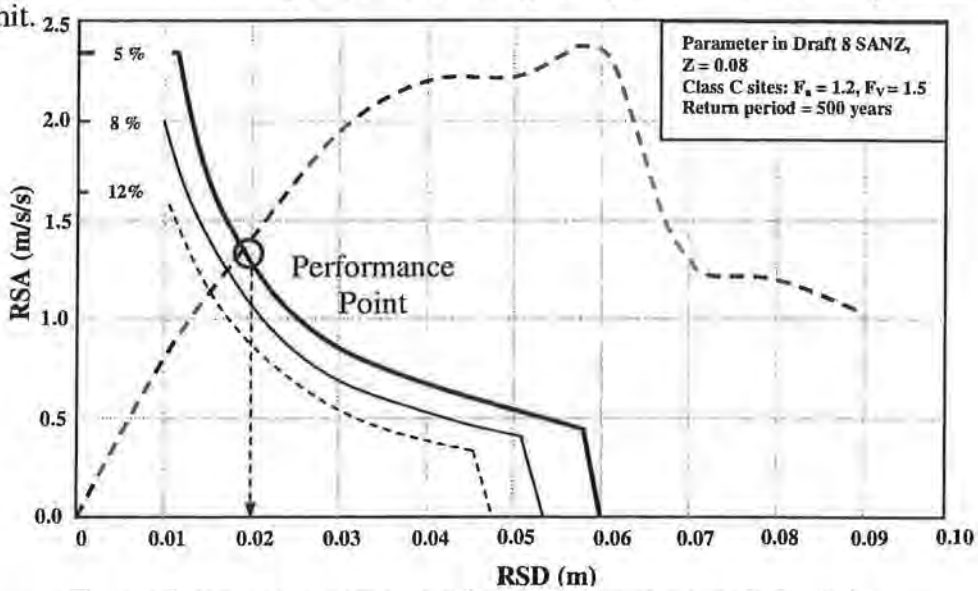

Figure 4. Capacity spectrum diagram of the case study building

4. ASSESSMENT OF ELEMENT PERFORMANCE

The shear capacities of the columns and possible "weak links" including beam-column joint failure have also been checked against the shear demand. In calculating the shear demand, the effects of the masonry infill have also been taken into account.

The shear capacity of the columns was estimated with reference to a multitude of code provisions including that of AS3600 [2001] and ACI-318 [2002] along with the well-known recommendations by Priestley et al. [1994] and Moehle et al. [2002]. The 500-year return period shear demands on the columns without masonry infill were found to be significantly less than the shear capacity.

The introduction of concrete cavity masonry infill wall panels between RC columns at ground level was found at a limited number of locations. The stiffening effect of the infill wall can be idealized as a diagonal strut that braces the portal frame until the wall strength is reached. This strut action could induce excessive local shear forces in the adjacent RC columns and result in the shear resistance of a few of the ground floor columns being exceeded. This was not considered critical to the overall stability of the building since alternative load paths exist in adjacent portal frames and the global response of the structure is displacement and not force controlled. In view of the limited displacement demand of the earthquake (20mm), the failure of a column in shear would not lead to the collapse of the building provided that the column is effectively braced by adjacent lateral load resisting elements, which perform satisfactory.

The shear capacity of the beam-column joints has also been assessed in accordance with the estimates of the forces that could be transmitted from the adjoining beams and columns. The resulting stress conditions associated with "joint opening" and "joint closing" actions have been analysed using the Mohr's circle approach based on recommendations by Priestley [1995]. This approach is preferred over the simplified method suggested by FEMA273 [1997], which does not explicitly account for the effects of axial pre-compression in the joint. The critical principal tensile and compressive stresses developed at the beam-column joints were found to be within the permissible limits in both tension and compression.

5. EXPERIMENTAL PROGRAM ON SOFT-STOREY COLUMNS

In this study, an experimental program on typical soft-storey columns will be undertaken to develop and verify the analytical column-deformation model. Cantilever column specimens representative of current constructional practices will be tested to study the force-displacement behaviour under both monotonic and cyclic loading. The typical experimental set-up is shown in Figure 5. The newly established *Digital Close-range Photogrammetry Technique* [Fraser, 1997] will be used for measuring deformation and surface strains. One of the key objectives of the experiments is to evaluate the accuracy of the analytical procedure in resolving deformation into the respective components including the contributions from flexure, shear and yield penetration.

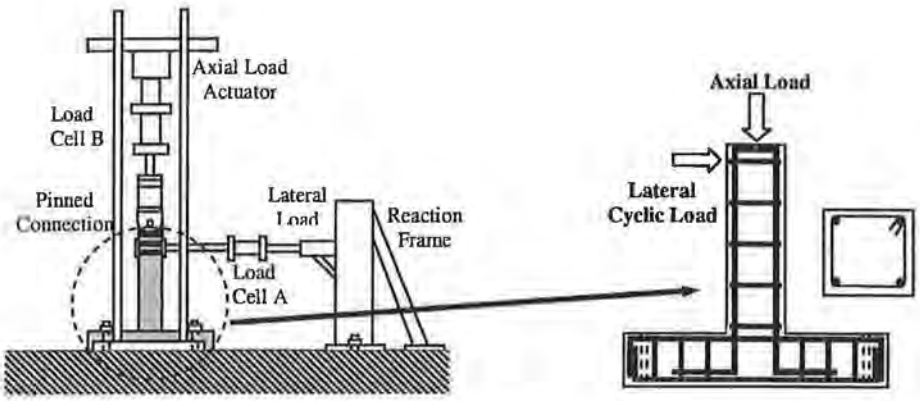

Figure 5. Experimental equipment for cyclic load test

6. CLOSING REMARKS

This paper presents the application of a simple and effective non-linear static procedure to evaluate the seismic performance of a soft-storey building by comparing the seismic demand with the capacity. The seismic demand is represented realistically by a recently developed response spectrum model plotted in ADRS format. The capacity of the soft-storey is ascertained using a deformation model that has accounted for the effects of axial compression, flexure, shear, column-end rotation and foundation flexibility. The uneven sharing of shear forces between the columns and the significant additional shear demand associated with the strut actions in the masonry infill are amongst the numerous important issues that have been raised for special attention. An experimental program is being planned to confirm the accuracy of the analytical procedure.

7. REFERENCES

ACI318 (2002) Building Code Requirements for Reinforced Concrete and Commentary, American Concrete Institute.

Alsiwat, M. and Saatcioglu, M., (1992) Reinforcement Anchorage Slip Under Monotonic Loading, Journal of Structural Engineering, Vol 118(9), pp 2421-2437.

AS/NZS 1170.4 Draft no.8 (2003) Structure Design Actions – Part 4: Earthquake Action, sub-committee BD/6/4, January.

AS1170.4 (1993) Minimum Design Loads on Structures: Part 4: Earthquake Loads.

ATC40 (1996) Seismic Evaluation and Retrofitting of Concrete Buildings, Applied Technology Council, USA.

FEMA273 (1997) NEHRP Guideline for the Seismic Rehabilitation of Buildings, Washington DC, Federal Emergency Management Agency, USA.

Fraser, C., (1997) Some Thoughts on the Emergence of Digital Close-Range Photogrammetry, President's Medal Address to the Photogrammetric Society, London.

Moehle, J., Elwood K. and Sozen, H., (2002) Gravity Load Collapse of Building Frames During Earthquakes, Special Publication, Uzumeri Symposium, American Concrete Institute, Farmington Hills, Michigan.

Panagiotakos, T. and Fardis, M., (2001) Deformations of Reinforced Concrete Members at Yielding and Ultimate", ACI Structural Journal Vol 98(2), pp 135-148.

Park, R. and Paulay, T., (1975) Reinforced Concrete Structures, Wiley.

Priestley, M., (1995) Displacement Based Seismic Assessment of Existing Reinforced Concrete Buildings, Proceedings of the Pacific Conference on Earthquake Engineering, Vol 2, pp 225-244.

Priestley, M., Verma, R. and Xiao, Y., (1994) Seismic Shear Strength of Reinforced Concrete Column, Journal of Structural Engineering ASCE, Vol 120(8), pp 2310-2329.

Vecchio, FJ., and Collin, MP., (1986) The Modified Compression Field Theory For Reinforced Concrete Elements Subjected to Shear, ACI Structural Journal, Vol 83(2), pp 219-231.

Watson, S., Zahn, F. and Park, R., (1994) Confining Reinforcement for Concrete Columns, Journal of Structural Engineering, ASCE, Vol 120(6), pp 1798-1824.

Wilson, J. and Lam, N., (2003) A recommended earthquake response spectrum model for Australia, Australian Journal of Structural Engineering, Institution of Engineers Australia, Vol5(1), [In press]

THE VITAL ROLE OF ENGINEERS IN URBAN SEARCH AND RESCUE

DAVID BRUNSDON AND DES BULL
KESTREL GROUP LTD, WELLINGTON, NEW ZEALAND AND HOLMES CONSULTING GROUP, CHRISTCHURCH, NEW ZEALAND

INVITED SPEAKER

AUTHORS:

David Brunsdon is the Immediate Past President of the New Zealand Society for Earthquake Engineering, and is the National Lifelines Co-ordinator. He is a Director of Kestrel Group Ltd, a risk & emergency management consulting practice, and a member of the NZ Urban Search and Rescue Steering Committee.
(db@kestrel.co.nz)

Des Bull is a Technical Director of Holmes Consulting Group, and the Holcim Adjunct Professor in Structural Engineering at the Department of Civil Engineering, University of Canterbury. He is the NZ Urban Search and Rescue Engineering Training Leader, and is also a member of the seismic loadings sub-committee of the Joint Australian and New Zealand Loadings Standard.
(desb@holmesgroup.com)

ABSTRACT:

Structural Engineers are a key part of an Urban Search and Rescue (USAR) response. They have a critical role to play in providing technical advice for rescue teams. This includes assessing the overall stability of a partially or wholly collapsed structure, monitoring the structural stability and the development of temporary shoring arrangements. To be fully effective in a rescue situation, engineers must be specifically trained in USAR procedures and techniques, and must have regular involvement with the rescue teams with which they are associated.

This paper summarises the key roles that engineers play in conjunction with a USAR rescue team, and outlines the arrangements currently being established with both the national Task Force teams and local rescue teams in New Zealand. Details of the new Level One and Level Two USAR Engineer training courses currently under development are provided.

1. INTRODUCTION

Urban Search and Rescue involves the location, rescue and initial medical stabilisation of victims trapped in confined spaces following a structural collapse. Such incidents can range from single site collapses through to multi-site situations resulting from landslides or earthquakes. Search for the injured and rescue of those trapped are among the most important and urgent post-earthquake activities. Those conducting USAR activities can themselves become victims, as a high level of risk is associated with these activities.

Engineers involved in USAR activities need to be comfortable dealing with high-pressure situations and able to make rapid decisions. A familiarity with disaster environments and the procedures of specialist rescue task forces needs to be developed. This familiarity requires specific prior training and engagement with emergency service agencies.

This paper describes the functions of an engineer in USAR activities, and outlines the contents of engineering training courses currently under development to enable New Zealand engineers to become effective in emergency events that involve USAR.

2. ENGINEERS AS A SPECIALIST USAR SKILL CAPABILITY

Engineers are a recognised specific specialist skill grouping in USAR, along with Paramedics and Search Dogs. The organisational structure set up by the New Zealand National USAR Steering Committee includes a Specialist Skills Working Group, the focus of which is the development of training material and operational mechanisms for these three groups.

The focus of the development of a USAR capability in NZ is on developing *regional capability* in terms of local rescue teams in parallel with a *specialist national capability* in the form of three Task Forces (Angus et al, 2003, and www.usar.govt.nz). The development objectives for the specialist skill groups reflect this approach, and can be summarised as:

- *At regional (local) level*
  - A group of Engineers, Search Dogs & Paramedics familiar with USAR processes (Category 1 – surface search and rescue) and able to assist the initial response
- *At Task Force (national) level*
  - Have at least two Engineers, Search Dogs & Paramedics assigned to each of the Task Forces and capable of operating at Category 2 level (confined space rescue)

The involvement of engineers from disciplines other than structural is also particularly important, as they can play a significant role in different types of collapse situation (for example, geotechnical engineers in landslide situations), and in the operational planning

and logistics support areas generally.

3. THE OPERATIONAL ROLE OF ENGINEERS IN USAR

The task of regionally trained engineers, first on the scene with local rescue teams, is likely to be structural triage – the setting of rescue priorities with respect to the risk posed by the partially or wholly collapsed structure.

The role of a Task Force engineer is to provide *critical information*, and not to make all the critical decisions (Hammond, 1995). Task Force leaders will consider the advice of the engineer along with others and develop their action plan for the rescue operations accordingly. The opinion of the engineer may not always be adhered to, and some aspects of a rescue will take place without the input of engineering advice.

The scope of the principal inputs required from a Task Force engineer can be summarised as:

- Assist in structural triage
  - *Prioritise which structures should be searched first in a multiple collapse situation; advise on safe routes for approaching the building; advise on building stability for planning and executing Search and Rescue (ie. determine safe staging areas and consider the likely void spaces where victims could be within the collapse)*
- Provide structural engineering advice
  - *Confirm Task Force decisions on shoring, cribbing, breaching and heavy lifting, when needed; specific design of shoring elements as requested.*
- Assist in the reduction of hazards
  - *Identify hazards; assist with the set-up and monitoring of systems for checking stability and hazard control, in support of the Safety Adviser.*

Task Force engineers need to be well prepared to make difficult decisions in an environment that is very different from the orderly design office. The environment during a USAR event is likely to be chaotic, with many uncertainties relating to the safety status of buildings and many traumatised people.

The engineer also needs to be aware of the roles of the other members of the Task Force. Most of the Task Force personnel come from rescue backgrounds and are used to making rapid, high-pressure decisions as part of their normal occupation, and will take a significant risk in order to save a life. Therefore a conflict in focus can arise between engineers and rescue workers – rescuers save victims, whereas engineers focus on rescue safety.

It is emphasised to Task Force technicians that each person is responsible for their own safety when exposed to a variety of hazards (chemical, biological and structural etc.). Task Force technicians need to be carefully instructed on hazard recognition and

mitigation. Engineers therefore have an important role in the training and preparation of USAR team members. Structural hazards include the range of typical collapse modes for different types of structures, along with the fundamentals of structural instability (what can a damaged structure do once it has come to rest; what will trigger further collapses; consideration of approaching and working on and in damaged structures) and the estimation of component masses, to list some aspects. Engineers are responsible for establishing sound skills for communicating engineering objectives, between the Task Force engineers and all other team members.

4. USAR TRAINING FOR NEW ZEALAND ENGINEERS

Work on creating a framework for training engineers to be able to effectively assist with minor and major building collapse incidents was initiated by research undertaken at the University of Canterbury (McGuigan, 2002). The framework features two components of training engineers in USAR – (i) *familiarity with how emergency services operate*, and (ii) *specialist engineering skills for collapse situations.*

A progressive training system is being developed, with the following key features:

Level 1 USAR Engineer

- *Outcome* – a regional (local) resource assisting (or part of) local volunteer rescue teams
- *Focus* - operating on the outer perimeter of building or site
- *Status* – IPENZ Engineers NZ–endorsed CPD course with 12 hours credit
- *Targets* – Graduate engineers and above who have completed *USAR Awareness*

Level 2 USAR Engineer

- *Outcome* – capable of operating with USAR Task Force teams
- *Focus* - operating within a structural collapse site (overall structure & element stability)
- *Status* – IPENZ–endorsed CPD course with 12 hours credit
- *Targets* – Chartered Professional engineers who have completed *Level 1 USAR Engineer* and obtained their Orange Card

The basic entry level USAR qualification is obtained from a 2-day unit standard training course *USAR Awareness* (Category 1A). Holders of this unit standard are issued a pocket-based Orange Ticket. For those wishing to become more actively involved, a USAR Responder Orange Card results from the completion of 3 additional courses totalling 5 days (including the First Aid certificate which ideally all engineers should have as a matter of course). The Orange Card features a photograph of the holder, and so provides an appropriate form of identification that addresses the often-raised question of how engineers and other supporting technical resources will obtain access

through perimeter cordons around major emergency sites.

The content of the *Level One USAR Engineer* course is shown in Table 1. This course is to be taught over a 24 hour period (an evening and the following day) at regional centres in New Zealand. This course is currently under development, with the aim of being available for delivery during the 2003/ 04 financial year.

The *Level Two USAR Engineer* course builds on material taught during Level One training and intends to give the participating engineer more knowledge to deal with collapsed structures and an understanding of how people perform in a real emergency. It is intended that the advanced USAR engineering course be delivered over the same 24 hour basis as for the Level One course, but taught from the Task Force bases. The course content is shown in Table 2. Task Force Engineers also need to participate in a three-day (72 hour) rescue simulation exercise alongside Task Force technicians before being eligible for selection. The relationship of these courses with the USAR category training system is outlined in a separate paper (Angus et al, 2003).

An engineer who participates in Task Force activities needs to have achieved Chartered Professional Engineer status, and will need to possess a number of personal attributes so that they are suitable for actual events. This includes a reasonable level of fitness due to the demanding nature of the exercise and the potential long hours that can be worked. The engineer will need to be adaptable and able to fit in to the structured nature of the Task Force operation. A good understanding of practical construction methods and some experience in construction and demolition related work is also expected.

5. USAR TRAINING FOR AUSTRALIAN ENGINEERS

Australia has been developing a USAR capability since the mid-1990's, working co-operatively with NZ. This work is currently being led by the National USAR Working Group (NUSARWG) under the leadership of Emergency Management Australia.

Task Forces including the Training and operational requirements are resourced on a state by state basis with guidance and support from the NUSARWG and the Australasian Fire Authorities Council. New South Wales, Victoria and Queensland have dedicated USAR Task Forces of varying levels of capability, and the other States and Territories are in the process of developing their USAR capacities

NSW are fortunate in having direct access to structural and other engineers employed by the NSW Department of Public Works & Services (DPWS). In a recent development, all civil and structural engineers taking up a position within the NSW DPWS have the requirement in their job description to undertake USAR Category 1 training. The broader NSW DPWS objective is to have two Category 2 engineers in each of their five principal regional offices.

The NSW USAR engineering module is based on four modules - *USAR Operations* (8 hours), *Effective Team Operations* (4 hours) *Remote Living Conditions* (4 hours) and

Practical Field Operations (12 hours as part of the 48 hour Technician Exercise). This course is essentially an induction course for Task Force members, with a strong operational focus.

Recent feedback from Australian USAR Task Force leaders and engineers in other states suggests that some of the technical modules of the New Zealand courses under development are of interest to them.

Table 1: Level 1 Engineering Course Outline

Module	Key Elements
Module 1.1 ***The USAR Training & Response Framework***	USAR organisational structures and Training Framework CIMS introduction/ refresher; Health & Safety context
Module 1.2 ***Role of the Engineer; Rescue Team Dynamics***	Role of the engineer at a USAR operation Understanding rescue team dynamics
Module 1.3 ***Site Technical Processes***	Building Triage Hazard Assessment and Building Marking
Module 1.4 ***Building Collapse Patterns***	Engineering issues in collapsed buildings - safety and stability
Module 1.5 ***Scenario: Role Playing/ Process Familiarity***	Single site collapse scenario
Module 1.6 ***Operational Issues***	Professional Indemnity & Personal Insurances

Table 2: USAR Level 2 Engineering Course Outline

Module	Key Elements
Module 2.1 ***Task Force Reality***	What does it mean to be part of a Task Force? Response and training expectations
Module 2.2 ***Human Response Issues***	The reality of how people perform in real emergencies
Module 2.3 ***Site Technical Processes I***	The design of shoring & bracing Hazard assessment/ reporting
Module 2.4 ***Site Technical Processes II***	Shoring & cribbing Breaching & cutting
Module 2.5 ***Hazard Mitigation*** ***Safety Equipment***	Advanced building monitoring techniques Hazard monitoring and gas analysis Use of search cameras and Trapped Person Locator Heavy (specialist) equipment
Module 2.6 ***Course Conclusion***	Recap on key points, next steps Discussion and course closure

6. OPERATIONAL ISSUES

There are many professional considerations associated with the operational involvement of engineers in USAR training and actual deployments. These include:

- Training obligations for the engineer
- Mobilisation mechanisms – response expectations
- Professional indemnity and public liability
- Health and safety responsibilities
- Remuneration

A specific agreement between professional engineers and the USAR Task Forces has been prepared to address this and other issues. This agreement is based on the invited individual engineers to be attached to the Task Forces by way of a standing secondment from their practice to the NZ Fire Service. This is seen as a way of creating a defined and renewable relationship between nominated individuals and the Task Forces which doesn't attract undue liability to either the individual or their practice. An honorarium which contributes towards the annual training and engagement time commitments is to be offered with this appointment.

The liability implications for engineers responding as part of local rescue teams or as individuals are still being worked through. While the new Civil Defence and Emergency Management Act provides cover for responders working under the direction of the Controller in a declared emergency, a local structural collapse situation (eg. single site) would however not result in a declared civil defence emergency, and the level of protection afforded to an engineer providing operational advice is unclear. This applies to engineers operating as either individuals (eg. outside working hours) or on behalf of consulting practices.

In any operational situation it is important to note that while the principal role of an engineer is to provide specific safety advice, the overall responsibility for Health and Safety must stay with the rescue team leader.

7. CONCLUDING OBSERVATIONS

Professional engineers are required to fulfil a vital role in rescue operations, assisting with critical decisions relating to the safety of operations and determining suitable methods to ensure temporary stability of collapsed structures. Engineers need to be specifically trained so that they can be effective in demanding and dangerous situations that are quite different from their normal working environment.

A two-level USAR training system for New Zealand engineers is being developed with the objective of providing a specialist engineering response capability at both regional and national levels. The training includes specific courses for engineers and courses involving participation with members of the emergency services. Technical modules from these courses are considered to be relevant and applicable to Australian engineers.

During USAR training, engineers will gain first-hand exposure of the nature of rescue operations and the personnel involved. Ongoing training will need to be undertaken to ensure skill levels are maintained. The USAR engineering courses will form a valuable continuing professional development module for practising engineers, by providing an opportunity for engineers to develop leadership skills and promote community awareness of the engineering profession.

While no amount of training can prepare people for the overall effects of a disaster scene, appropriately focused training for specialist skill personnel such as engineers is essential and will go a long way towards giving engineers a better idea of what to expect.

References

Angus, L. B., Dance, R. J. & Brunsdon, D. R. 2003. *Developing an Urban Search and Rescue Capability for New Zealand: Two Years of Achievements*, Proc. of the Pacific Conference on Earthquake Engineering, Christchurch, February 13-15, 2003.

Hammond, D. 1995. *"Engineering" the Collapse: Making the Structure Safe*, Fire Engineering Journal, Vol 148 (11) 49-63.

McGuigan, D. M. 2002. *Urban Search and Rescue and the Role of the Engineer.* Masters of Engineering Project Report. University of Canterbury, Christchurch.